`

PNIPAAM IMMOBILIZED NANOPARTICLES FOR POSTERIOR SEGMENT OCULAR DELIVERY

PNIPAAM IMMOBILIZED NANOPARTICLES FOR POSTERIOR SEGMENT OCULAR DELIVERY

By, PAYAL, B.Tech.

A Thesis Submitted to the School of Graduate Studies in Partial Fulfillment of the Requirements for the Degree Master of Applied Science in the School of Biomedical Engineering

McMaster University

Master of Applied Science (2020) McMaster University
School of Biomedical Engineering Hamilton, Ontario

TITLE: PNIPAAM IMMOBILIZED NANOPARTICLES FOR POSTERIOR SEGMENT OCULAR DELIVERY

AUTHOR: PAYAL, B.Tech. (GRIET, Hyderabad, India)

SUPERVISOR: Dr. Heather Sheardown, Dr. Varun Chaudhary

NUMBER OF PAGES: xii , 65

ABSTRACT

Ocular drug delivery to the posterior segment of the eye is extremely challenging. The delivery of the pharmaceuticals is made difficult by the numerous barriers that are present in the eye, as well as the isolated nature of the eye. The eye also consists of efficient drainage routes that eliminate the drug that has entered the eye successfully. Because of these reasons, drug delivery to the posterior segment of the eye is challenging and complicated. As a result, conventional eye drops are an inefficient way to deliver the pharmaceuticals to the eye as <5% of the administered dose is delivered to the anterior segment of the eye, and a negligible amount is delivered to the posterior tissues. The work presented in this thesis focuses on the design, synthesis, and characterization of the PLGA nanoparticles as a drug delivery vehicle to treat diseases associated with the posterior segment of the eye. The slow-release formulation was developed using PLGA nanoparticles and synthesized by the Double Emulsion Method (W_1-O-W_2). The PLGA nanoparticles were optimized by following various protocols and formulations to obtain the highest encapsulation efficacy and desired particle size range by changing the intensity of sonication, speed of ultracentrifugation, composition, and amount of the stabilizer and PLGA nanoparticles. The nanoparticles showed a 97% encapsulation efficiency with Bovine Serum Albumin (BSA) and a particle size of 201 nm. The slow-release formulation was further developed by immobilization of the particles in a thermogelling PNIPAAM scaffold. In vitro drug release results suggest that PNIPAAM containing PLGA nanoparticles produced in this work has the potential to be further developed and used as a drug delivery vehicle for the posterior segment of the eye.

ACKNOWLEDGMENTS

I want to thank my supervisor Dr. Heather Sheardown for her continuous support and guidance throughout my research. As an international student, it was overwhelming when I first moved to Canada for the MASc, but Heather made sure I was doing okay and made friends. She always reached out to me, and without her support, this thesis would not have been possible.

I also want to thank my co-supervisor, Dr. Varun Chaudhary, for his support and advice during this project. I would also like to thank my committee members, Dr. Boyang Zhang and Dr. Leyla Soleymani.

I would also like to thank everyone in the Sheardown Lab for their continuous feedback during Lab presentations; without the advice, I would not have completed this research. I want to thank Lina for helping me with the project and training me on many instruments and special thanks to my friend Karim Soliman who has been the most significant support and always was a call away and provided with insights throughout the research. Thank you so much for answering all my questions and helping me always.

A massive shoutout to everyone in the Sheardown group and specials thanks to Talena, Mitch, Nicole, Aakash, Jennifer, and Taylor for making my graduate experience a memorable one.

Next, I want to thank my friend Prithwiraj for supporting me always. Lastly, I want to thank my brother, Krishna, for always supporting and motivating me throughout my life. I do not know what I will be doing without you. Thank you to Suman Aunty for treating me like her child always. To my mother, thank you so much for your endless love, sacrifice, and support and for believing in me. No words in this world are enough to describe the love that I have for my late father. There is not a single day that I do not miss you, Papa. Thank you so much for all the love and blessings you have given me, and I miss you and love you a lot.

TABLE OF CONTENTS

LIST OF FIGURES

CHAPTER 2

CHAPTER 4

CHAPTER 7

LIST OF TABLES

CHAPTER 2

CHAPTER 3

CHAPTER 4

LIST OF ABBREVIATIONS AND SYMBOLS

PLGA	Poly(lactic-co-glycolic acid)
AMD	Age-related Macular Degeneration
DR	Diabetic Retinopathy
DME	Diabetic Macular Edema
RPE	Retinal pigmented epithelium
PLA	Polylactic Acid
PGA	Polyglycolic Acid
TGF-β2	Transforming growth factor-β2
PNIPAAm	Poly(N-isopropylacrylamide)
ECT	Encapsulated Cell Technology
CNTF	Ciliary Neurotrophic Factor
RP	Retinitis Pigmentosa
GCV	Ganciclovir
CMV	Cytomegalovirus
MEMS	Microelectromechanical System
wAMD	Wet Age-related Macular Degeneration
VEGF	Vascular Endothelial Growth Factor
CNV	Choroidal Neovascularization
FDA	Food and Drug Administration
T_g	Glass transition temperature
$W_1/O/W_2$	$Water_1/Oil/Water_2$
BSA	Bovine Serum Albumin
PBS	Phosphate Buffer Saline
DCM	Dichloromethane
PVA	Poly Vinyl Alcohol

CHAPTER 1: INTRODUCTION

Ocular drug delivery is exceptionally challenging because of the numerous physical and anatomical barriers that are present in the eye. Topical drug delivery is an inefficient way to deliver the pharmaceuticals to the eye as <5% of the topically applied drugs get absorbed by the intraocular tissues and reach the anterior segment, and a negligible amount of the drug enters the posterior segment of the eye [1]. Systemic drug administration is also limited in its ability to deliver the therapeutics to the posterior segment of the eye as only 1-2% of the systemically applied doses reach the posterior segment by crossing the blood-retinal barrier [2]. Periocular drug delivery involves the delivery of the pharmaceuticals to the tissues surrounding the eye, allowing the sustained release of pharmaceuticals to the posterior tissues [3]. However, the requirement for the drugs applied to the surface of the eye to cross the restrictive barriers to reach the posterior region makes it extremely challenging [1]**.** Intravitreal Injection through the pars plana in the eye is the most effective method of delivering therapeutics to the posterior segment of the eye. This mode of delivery is advantageous as it can achieve high drug concentrations, and the administration is relatively easy [4]. However, due to efficient clearance mechanisms that are present in the eye, frequent injections are needed to maintain therapeutic concentrations within the vitreous [5]**.** Frequent injections into the vitreous chamber of the eye lead to undesirable side-effects. Polymeric nanoparticles can be used as drug delivery modalities to treat the diseases associated with the posterior segment of the eye, such as Age-related macular degeneration, a disease associated with the posterior segment of the eye because of their size, solubility, stability, and prolonged retention time**.** PLGA, poly-D, L-lactic-co-glycolic acid has been extensively used for ocular delivery; it has been approved by the US FDA as a "clinically applicable material" as it is biocompatible, degradable, and non-toxic [6]. PLGA

nanoparticles degrade by hydrolytic cleavage of the backbone ester linkages into two distinct entities, i.e., lactic acid and glycolic acid. As both the lactic acid and glycolic acid are endogenous acid metabolites, the monomers enter the Krebs Cycle. They are quickly metabolized in the human body to H_2O and CO_2 [7]. The degradation by-products are eliminated from the body through feces, respiration, and urine [8].

1.1 Thesis Objective

In this thesis, the synthesis of PLGA nanoparticles to deliver the therapeutics to the posterior segment of the eye is discussed. The project's primary focus is the design, synthesis, and characterization of PLGA nanoparticles and to investigate the benefits of nanoparticles as drug delivery modalities for posterior segment eye diseases. Additionally, a poly (N-isopropyl acrylamide) (PNIPAAM) thermogelling scaffold developed in the Sheardown lab was used to immobilize the nanoparticles. It is hypothesized that the incorporation into a gelled scaffold will result in a slow-release formulation that can increase the drug residence at the site within the vitreous chamber, thereby increasing the time between the injections.

1.2 Thesis Outline

The work in this thesis is divided into five chapters. The introduction, objective, and outline of this thesis are included in Chapter 1. Chapter 2 is the literature review of the numerous routes of drug delivery to the eye and the current therapies for the posterior segment eye diseases. Chapter 3 describes the materials and methods used in this research, and Chapter 4 describes the results from the design, synthesis, characterization, and drug release studies of the nanoparticles. Conclusion and Future Work of the thesis will be discussed in Chapter 5.

CHAPTER 2: LITERATURE REVIEW

2.1 THE EYE

Drug delivery to the eye is complicated by its isolated nature and the numerous barriers that are present. The eye is divided into two regions: the anterior segment and the posterior segment (Figure 1). The anterior region of the eye consists of lens, cornea, ciliary body, and aqueous humor while the retina, vitreous body, sclera, and the choroid comprise the posterior region. The posterior region of the eye makes up two-thirds of its volume. The structure of the eye is essentially that of a globe containing three concentric layers. The outermost layer of the eye is known as the fibrous tunic and is separated into cornea and sclera. The middle vascular layer consists of the ciliary body in the anterior chamber and choroid in the posterior chamber. The outermost and the middle layer are responsible for nutrition in the eye. Lastly, the innermost layer is composed of the neural retina. These concentric layers have gel-containing reservoirs present within them [9].

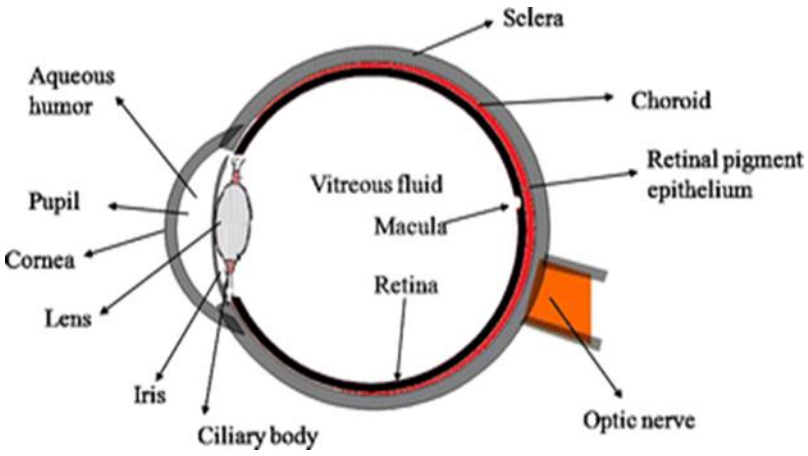

Figure 1: Basic anatomy of the eye [2].

Any pharmaceuticals must bypass all these concentric layers in order to reach the posterior segment. In addition to the barriers, the eye consists of efficient drainage mechanisms that remove any therapeutic that enters the ocular environment.

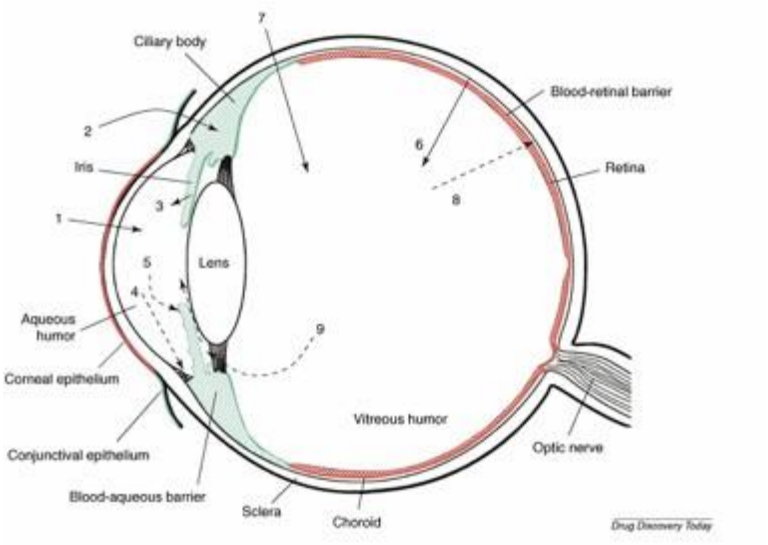

Figure 2: Different routes of drug delivery into the eye (solid arrows) and the efficient clearance mechanisms from the eye (dotted arrows). These different routes play a crucial role in determining the route of drug delivery to the eye [10].

There are numerous routes through which the drug can enter and be removed from the eye. Drugs can penetrate the anterior chamber of the eye by topical administration through transcorneal permeation (arrow 1) and the noncorneal permeation (arrow 2). In noncorneal permeation, drug diffusion is across the conjunctiva and sclera into the anterior uvea. Drugs can also pass through the blood-aqueous barrier and enter the anterior chamber with systemic circulation (arrow 3). Elimination from the anterior chamber occurs by the constant turnover of the aqueous humor to the trabecular meshwork and Schlemm's canal shown by arrow 4 or via the

systemic circulation across the blood-aqueous barrier as shown by arrow 5.

In the posterior chamber, drugs can enter by crossing the blood-retinal barrier (arrow 6) or by direct intravitreal injection/insertion. Typically, less than 5% of topically applied drug reaches the posterior eye, and therefore this is not considered an effective means of drug delivery. Elimination from the posterior region of the eye can be via two methods:- via the posterior route (arrow 8) across the blood-retinal barrier and in the anterior direction (arrow 9) [10]. The properties of the eye can be used to tailor the drugs according to their administration routes and address different ocular diseases.

2.2 ROUTES OF OCULAR DELIVERY

2.2.1 Topical Administration

The traditional method of treating anterior segment diseases is eye drops due to the ease of administration and low cost. With this administration method, the majority of the topically applied drug is lost due to precorneal losses such as tear dilution, lacrimation, tear turnover, and drainage that results in extremely low bioavailability, particularly in the posterior eye [2]. Because of the various barriers that are present in the eye, topical drug administration is an inefficient way to deliver the pharmaceuticals to the eye, with as much as 95% of the instilled drug being lost within the first five minutes following instillation [1]. The volume of eye drops (25-50 µl) typically administered to the patients is significantly higher than the capacity of the conventional sac (10 µl), resulting in significant losses to the eyelids and cheeks [11]. Due to these reasons, topical administration is typically used to treat diseases associated with the anterior eye as a negligible quantity of drug enters the posterior segment. Although much of the drug instilled is lost, topical eye drops remain a common and beneficial method for treating

ocular conditions, particularly those of the anterior eye, due to the high concentration and frequent administration of a drug that occurs.

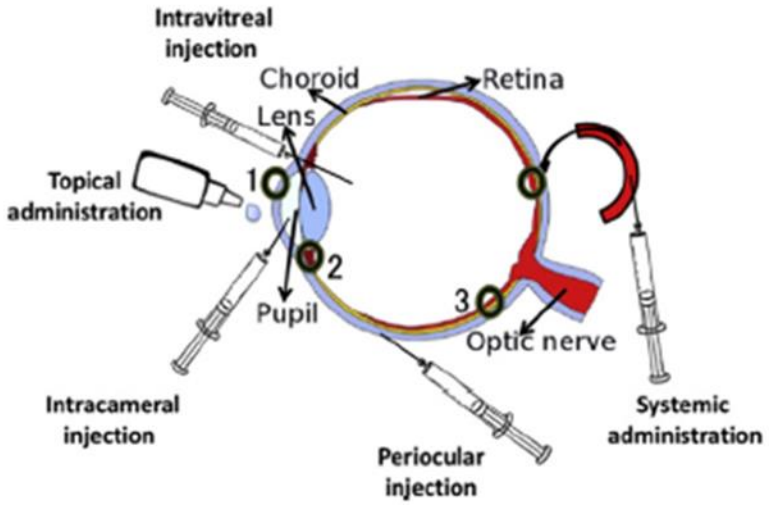

Figure 3: Routes of drug administration and barriers to drug delivery: 1- Corneal Barrier, 2- Blood-aqueous Barrier, and 3- Blood-retinal barrier in the eye [12].

2.2.2 Systematic Administration

Systemic drug administration is rarely used to deliver the therapeutics to the posterior segment of the eye since only 1-2% of the drug can cross the blood-retinal barrier [2]. Due to the low bioavailability of the drug, large doses are needed to maintain therapeutic concentrations. These large doses and the need for repeated administration, which is linked to side effects [13], make this an ineffective posterior segment drug delivery method. Therefore, diseases of the back of the eye are challenging to treat using conventional methods.

2.2.3 Periocular Delivery

Periocular delivery involves using subconjunctival injections into the subconjunctival space to form a localized depot, allowing the sustained release of pharmaceuticals to the

posterior tissues [3]. Periocular delivery also involves retrobulbar, peribulbar, and posterior subtenon injections. The advantage of this method is that it is less invasive than intravitreal injections [5] and has high patient compliance. It involves the delivery of the drugs to the tissues surrounding the eye. The drug is applied near the sclera resulting in high concentrations in the vitreous [2]. Periocular delivery has advantages over systemic administration as it has no systemic side effects. Nevertheless, the requirement for drugs applied to the surface of the eye to cross the restrictive barriers to reach the posterior region makes it extremely challenging [1].

2.2.4 Intravitreal Injections

Direct injection of the drugs through the pars plana is the most effective method of delivering therapeutics to the posterior segment of the eye. This mode of delivery is advantageous as it can achieve high drug concentrations, and the administration is relatively easy [4]. The retention time of the drug in the vitreous can be enhanced by increasing the molecular weight of the drug. Many drugs have a molecular weight of less than 500 Da resulting in an expected half-life of three days or less. On the contrary, protein therapeutics have half-lives on the order of a month. As a result, frequent injections are needed to maintain the therapeutic concentrations within the vitreous [5]. There are numerous risks associated with frequent injections such as retinal detachment, vitreal hemorrhage, cataract, and endophthalmitis [13]. The advantage of the drug delivery to the vitreous humor is that the volume of the human vitreous, at around 4 mL, represents approximately 80% of the volume of the eye and acts like a gel reservoir, providing a path to deliver implants or colloidal delivery systems with fewer side effects [9]. Smith et al. have shown that when the injections are given in the proximity of retinal breaks, the risk of retinal detachment is increased. There are a few globe-salvaging therapies performed in patients like ocular hypothermia, cryotherapy, radiation, and laser therapy, yet the

underlying difficulty is with injections itself [14]. Colloidal drug delivery systems offer a potential avenue for sustained release of pharmaceuticals in the vitreous, thereby maintaining required therapeutic concentrations. Polymeric microspheres like poly(lactic-co-glycolic) acid (PLGA) have been beneficial to deliver the drugs to the vitreous and retina, and the formulations are compatible with the ocular tissues [13]. Many current therapies for the treatment of posterior segment eye diseases utilize an intravitreal mode of injection to increase the drug residence time within the vitreous with minimal adverse side effects. However, there remains a need to decrease the frequency of injection and increase ocular residence time.

2.3. CURRENT THERAPIES FOR POSTERIOR SEGMENT DISEASES

Due to the various anatomical and physiological barriers present in the eye, and the efficient drainage mechanisms, delivery of the drug to the posterior segment of the eye is difficult. Intravitreal injections are given directly into the vitreous. As discussed, the drugs have a relatively short half-life in vivo, and repeated injections are required, which has the potential to lead to severe side-effects. The current drug delivery modalities focus on the sustained release of pharmaceuticals to treat diseases associated with the posterior eye, including age-related macular degeneration (AMD), diabetic retinopathy (DR), and glaucoma. Current therapies include implantable scaffolds, particles, iontophoresis, and in situ gelling systems. The goal is to provide sustained release of drugs within the vitreous, thereby reducing the number of injections and side-effects.

2.3.1 Implantable Devices

The significant volume of the vitreal chamber makes it an obvious choice to achieve

sustained release. The most accepted methods of posterior segment drug delivery involved the use of implantable scaffolds, including Retisert, Vitrasert, Ocusert, Iluvien, and iVation [15]. Several of these have been commercialized. These implantable scaffolds can be either degradable or non-degradable, with non-degradable devices offering the advantage of prolonged-release periods but remain in the eye. Iluvien, for example, an implantable non-degradable device that is inserted into the vitreous cavity, releases fluocinolone acetonide to the retina for 36 months to treat Diabetic Macular Edema (DME). As this implant is non-degradable, it remains in place after the release is completed. While not common, side effects include migration to the anterior chamber and results in dislocation [16].

In contrast, bioerodible devices have gained prevalence, as no surgical intervention is required to remove them. These implants can be eliminated from the body, thereby improving patient convenience [13]. In some cases, bioerodible implants have been shown to have a final uncontrollable burst release that can result in side effects [1].

2.3.2 Particles

Sustained release of the pharmaceuticals can be achieved without surgical intervention or repeated injections by incorporating the drug into microparticles (1-1000 μm) or, more preferably, nanoparticles (1-1000 nm) [17]. Bourges et al. have shown that after a single intravitreal injection, nanoparticles can be seen in RPE cells after four months, indicating that nanoparticles can be used for sustained drug release [1]. In many cases, microparticles and nanoparticles are formulated using polylactide (PLA), polyglycolide (PGA), and poly(lactide-co-glycolide) (PLGA) copolymers as they are biocompatible and biodegradable [18]. The size of the nanoparticles plays a vital role in determining the degradation pattern. Particles >10 μm in

diameter cannot undergo phagocytosis and thus elicit a foreign body response, whereas particles <5 µm in size undergo phagocytosis, resulting in rapid degradation [19]. The downside of nanoparticulate based systems is the propensity to induce vitreal clouding [20]. Nanoparticles were formulated with tamoxifen-induced inflammation in rats without exhibiting any toxicity [20]. However, the most significant hurdle with nanoparticles is that the lack of knowledge on the interaction of the particles with living tissues and cells [21]. There are several different nanoparticulate based systems, including micelles, nanoparticles, dendrimers, and liposomes.

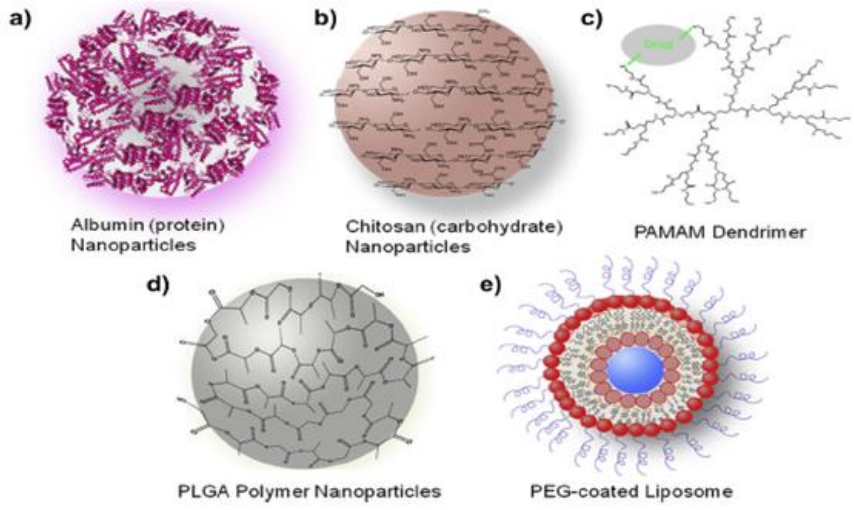

Figure 4: Nanoparticulate based systems used as drug delivery modalities for ophthalmic use [4].

Liposomes are lipid-based vehicles with a diameter of 25-1000 nm in size that enhance the half-life of drugs. In the back of the eye, they are engulfed through phagocytosis by retinal pigmented epithelium (RPE) cells. Liposome technology was used to make Visudyne by Novartis to treat choroidal neovascularization and age-related macular degeneration [1]. Liposomes can be prepared by various preparation methods with varying sizes, stability, and drug release kinetics [1]. Liposomes can encapsulate both hydrophilic drugs and lipophilic drugs. The hydrophilic

drugs can be incorporated in the core, whereas lipophilic drugs can be uptaken by the aqueous interior of the lipid bilayer [4]. The significant drawbacks of liposome as a drug delivery vehicle include high cost, rapid removal from blood by cells, vitreal clouding after the injection into the eye, and leakage of the encapsulated drugs [6].

2.3.3 Iontophoresis

Iontophoresis is convenient and non-invasive, enhancing drug penetration to the anterior and posterior segments of the eye. It utilizes ionized drugs that are carried through ocular barriers with the aid of electric current. There are three different types of iontophoresis: 1) trans-corneal 2) trans-scleral and 3) corneoscleral [1]. To deliver drugs to the posterior segment of the eye, the trans-scleral iontophoresis method is most used. There are various iontophoresis devices currently undergoing clinical trials. One of them is the Eyegate II delivery device, a needleless process that maintains the therapeutic concentration of the drug by direct administration into ocular tissues [1]. Esther et al. found that after a single transcorneal iontophoresis for 1 minute (1 ma), the dexamethasone level in the cornea of the rabbit eye was up to 30 fold higher compared to that were obtained after instillation of the eye drops [22]. Although iontophoresis is less invasive than intraocular injections, the duration of the drug activity is less compared to that of prolonged controlled drug release systems. As a result, repeated administrations are required [1], making it a less attractive choice due to low patient compliance and convenience.

2.3.4 In Situ Gelling Systems

This approach achieves the sustained release of pharmaceuticals to the posterior segment of the eye by using phase changing polymers [1]. These phase changing polymers are typically liquid at room temperature and form a gel at physiologic conditions. It is a useful method to

deliver drugs through intravitreal injections. For the delivery of therapeutics, the polymer undergoes a (phase) transition in the eye, forming a gel and gradually releasing the therapeutic from the solid depot over weeks or months. The factors that affect the phase transition are pH, temperature, light, or ion concentration [1]. The Sheardown Lab has developed a copolymer thermogelling scaffold based on PNIPAAm for posterior segment ocular delivery currently used in this research [23]. There are several stimuli-responsive materials currently being researched for posterior segment ocular delivery. A simple injectable hydrogel system was developed based on PEG and a vitamin E (Ve) methacrylate copolymer via hydrophobic phase separation for posterior segment ocular delivery. The hydrogels are formed in the aqueous environment with controllable kinetics driven by phase separation and polymer chain rearrangement, which is a spontaneous process depending upon the water uptake. The hydrogels can be customized to have desired characteristics like mechanical strength, water content, and drug release kinetics by varying the formulation of PEGMA-co-Ve polymer with an appropriate solvent or by changing the molecular weight of the polymer [24]. A controlled drug delivery polymer scaffold-like hyaluronic acid photogels can undergo crosslinking and de-crosslinking by altering UV light exposures [25]. These in situ gelling systems are a novel means of delivering drugs to the posterior segment of the eye.

2.3.5 Scleral Plugs

Several biodegradable scleral plugs have been used for vitreoretinal drug delivery. The scleral plugs are loaded with drugs and are implanted into the vitreous chamber of the eye. The plugs, comprised of PLA or PLGA, show sustained release of the pharmaceuticals over several weeks or months [13]. PLGA or PLA is used to make scleral plug implants for ocular diseases.

The PLGA scleral plug loaded with ganciclovir (GCV) was implanted at the pars plana to treat cytomegalovirus (CMV). The therapeutic release of GCV occurred for several months to a year in the vitreous [26]. As PLGA shows a triphasic drug release pattern, the release of GCV from the degradable scleral implant depends on the initial burst, the molecular mass, and composition of the PLGA, and a final burst phase as the implant undergoes bulk and surface erosion [13]. Several scleral devices, like coated coil matrix and the scleral implant composed of a refillable reservoir, has been invented [27].

Scleral discoid devices are used to treat the posterior segment eye diseases as they exhibit exceptional ocular biocompatibility with few side effects. As intrascleral devices are inserted through the periocular space, there is no perforation of the eyewall. The disadvantage of the scleral discoid devices is that the drug release has been shown to occur for only four weeks. Since it is implanted in the eye periocularly, the drug must first enter the eye and then pass through the restrictive ocular barriers making the drug release extremely difficult [13].

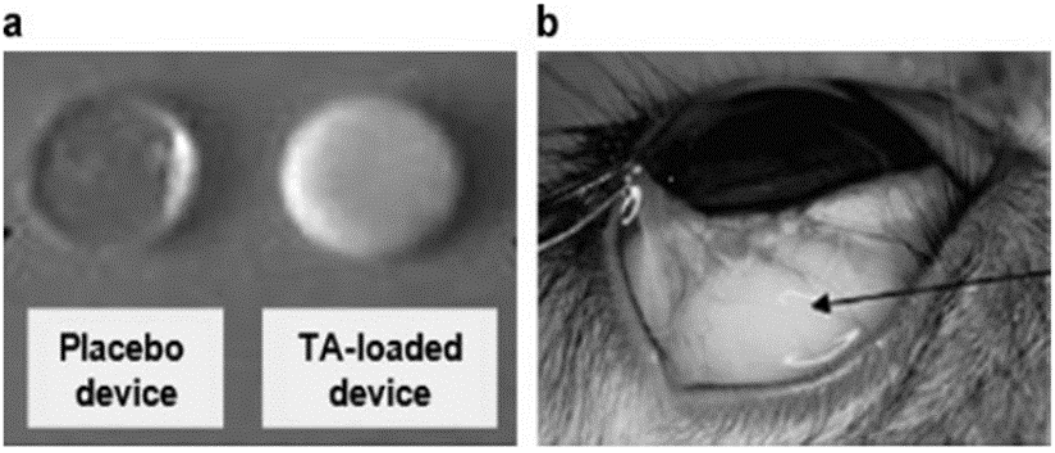

Figure 5: Scleral discoid devices implanted through periocular delivery in the beagle dog eye model [13].

2.3.6 Microelectromechanical Devices

Microelectromechanical devices (MEMS) provide a unique choice for the delivery of drugs to the eye. MEMS systems use micron-scale structures, and the systems can be implanted on the surface of the eye. The drugs are loaded into wells, and the therapeutic release occurs through the cannula or microneedle arrays; the potential for on-demand drug release also exists [28]. Jason et al. have shown that microneedles can pass through the sclera, and 10-35 µl of the fluid can reach the ocular tissues [29]. The newly developed MEMS devices are refillable such that the drug can be released for a prolonged period without the need for surgical interventions. The transscleral cannula can deliver the drug directly to both the anterior and posterior segments of the eye, and 250 nL of the drug can be delivered to the target tissues as the flow rate is applicable for ocular drug delivery [13].

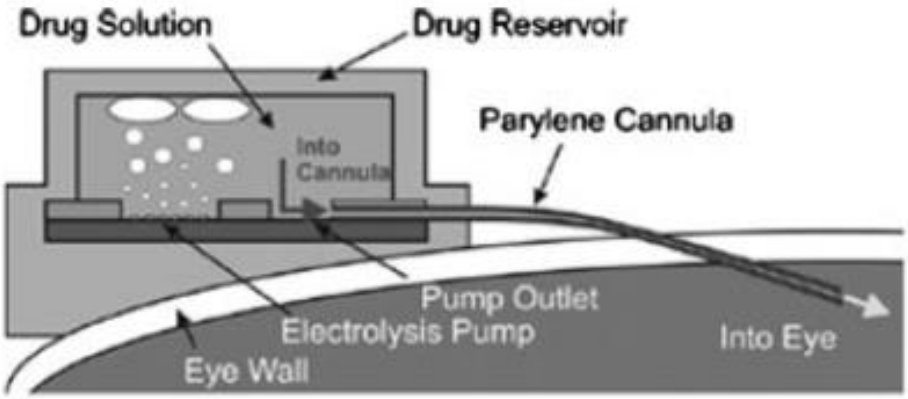

Figure 6: Micro-electromechanical drug delivery system showing drug delivery into the eye by electropumping [13].

2.4. Age-Related Macular Degeneration (AMD)

Age-related macular degeneration is the chief cause of irreversible blindness in the developed world, affecting people over 50 years of age and older [30].

AMD is generally classified into three types:

1. Early AMD
2. Intermediate AMD
3. Advance or Late Stage AMD which is further classified as:

a. Non-Neovascular AMD (Dry, Atrophic, or non-exudative AMD)

b. Neovascular AMD (Wet or exudative AMD)

With age, Bruch's membrane shows an accumulation of focal deposits known as Drusen due to incomplete clearance from the choriocapillaris [31]. The first clinical hallmark of AMD is the presence of Drusen. Early AMD is identified by the appearance of <20 medium-sized drusen. Intermediate AMD is distinguished by one large druse (>124 µm) and numerous medium-sized drusen (63µm to 123µm) as well as geographic atrophy [30]. Late-stage AMD is further categorized into two types: dry AMD and wet AMD.

The first clinical hallmark for the "wet" form of AMD is choroidal neovascularization (CNV), at which point there is an abnormal growth of blood vessels that are formed newly from the choroid to the Bruch's membrane. Neovascular AMD is characterized by the leakage of blood or plasma from the poorly constructed new blood vessels into the surrounding tissues that ultimately results in rapid vision loss [32].

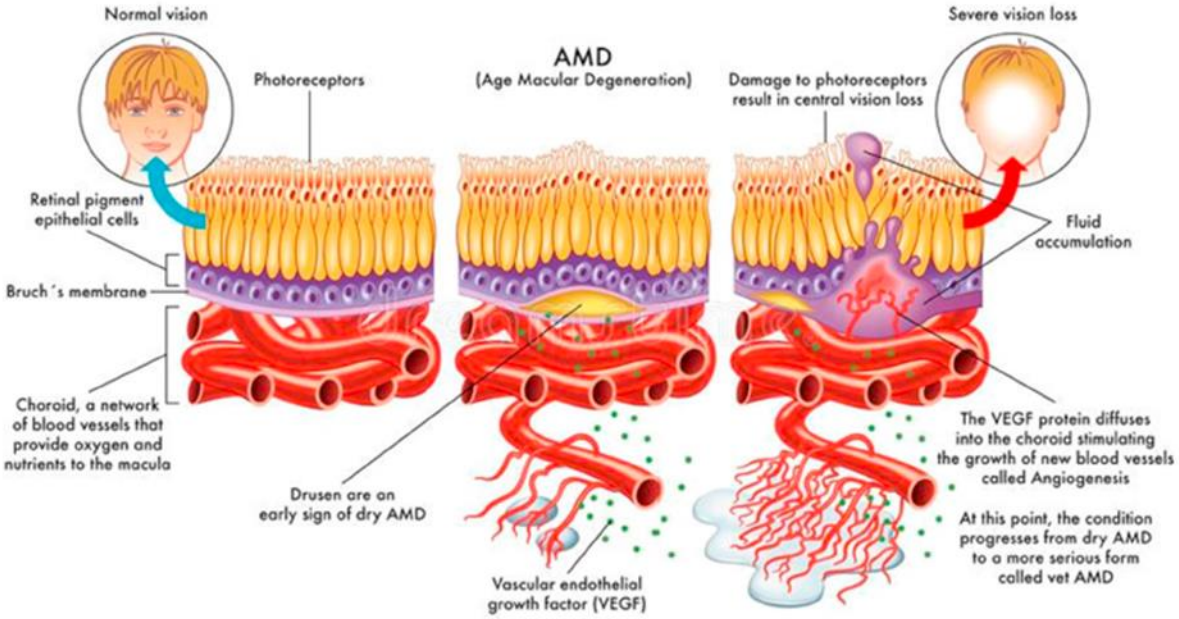

Figure 7: Schematic representation of Age-related macular degeneration [33].

The factors responsible for the definite diagnosis of AMD are Drusen formation, alteration of Bruch's membrane and RPE cells, choroidal neovascularization, and inflammation [34]. The other risk factors associated with AMD include genetic variations or the dysfunction of the RPE cells mediated by oxygen deprivation to form vascular endothelial growth factor (VEGF) that finally results in the development of CNV [34]. VEGF is a diffusible glycoprotein that stimulates new blood vessel formation. However, patients with early and late-stage AMD have increased expression of VEGF in the vitreous and the RPE [35]. $VEGF_{165}$ is the most potent of all VEGF isoforms and causes neovascularization, leading to retinal development [36]. Since VEGF has been associated with numerous ocular diseases, there has been extensive research with anti-VEGF therapies to treat neovascular diseases, including diabetic macular edema (DME), wet AMD, and CNV [37].

2.4.1 Current Anti-VEGF Therapies

At present, there are three anti-VEGF therapies available to treat neovascular AMD: Aflibercept (Eylea), Bevacizumab (Avastin), and Ranibizumab (Lucentis) [38]. The US Food and Drug Administration (FDA) has approved both Eylea and Lucentis to treat AMD [38]. Avastin is a monoclonal antibody and also an anti-VEGF agent approved by the FDA for the treatment of colorectal cancer [39] but is also used *off-label* to treat neovascular AMD [38].

2.4.1.1 Aflibercept (Eylea)

Eylea, co-developed by Regeneron and Bayer, is a fully human, recombinant fusion protein, commonly known as VEGF Trap-Eye, approved by the FDA in 2011 to treat wet AMD [40]. Aflibercept comprises of the binding domains of human VEGFR 1 and 2 fused to the Fc portion (Constant region) of human IgG1 [40]. It binds to all the isoforms of VEGF-A, VEGF-B, and placental growth factor (PIGF) with high affinity. Eylea is known as VEGF Trap-Eye because it acts as a soluble decoy receptor and binds to VEGF-A with high affinity, thereby inhibiting its interaction with VEGFR-1 and VEGFR-2 as these receptors are known to be activated by VEGF-A and lead to neovascularization [41]. The size of Eylea is 115 kDa resulting in an intravitreal half-life of 7.1 days and prolonged retention time expected to exceed 2.5 months [42].

2.4.1.2 Ranibizumab (Lucentis)

The US FDA approved Lucentis for the treatment of wet AMD in 2006. It is a humanized recombinant antibody fragment that targets all the isoforms of VEGF-A [38].

Lucentis is a chimeric compound consisting of a non-binding human sequence and an epitope derived from mice and has a high affinity to bind to VEGF-A [43]. In a two-year trial conducted to determine the efficacy of Lucentis for the treatment of wet AMD, 716 patients with Wet AMD received intravitreal injections of the drug at a dose of either 0.3 mg or 0.5 mg or placebo injections. At a 12-month time point, 95% of the patients lost fewer than 15 letters, thereby maintaining the visual acuity. Additionally, 25% of the 0.3 mg group and 34% of the 0.5 mg group showed visual improvement characterized by gaining 15 or more letters at 12 months. At a 24-month time point, patients receiving intravitreal injections with either dose of Lucentis showed a significant decrease in vision loss. Improved visual acuity of 6.5 letters was observed in patients receiving 0.3 mg dose of Lucentis and 7.2 letters in patients receiving 0.5 mg dose of Lucentis [44].

2.4.1.3 Bevacizumab (Avastin)

Avastin is a full-length humanized recombinant antibody that is approved by the FDA for colon cancer. It targets all the isoforms of VEGF and is used *off-label* to treat posterior ocular diseases like age-related macular degeneration (AMD) and diabetic retinopathy (DR) [38]. $VEGF_{165}$ consists of two binding sites- a heparin-binding site and a receptor binding site. Lucentis and Avastin bind directly to the receptor-binding domain of VEGF and inhibit VEGFR signaling by themselves [45]. In a trial conducted to determine the efficacy of Avastin (1.25 mg) and Lucentis (0.5 mg) to treat wAMD, 1208 patients with wet AMD received intravitreal injections monthly or as required. After one year, the patients treated with a dose of 1.25 mg Avastin gained eight letters. Patients treated with a dose of 0.5 mg Lucentis monthly gained 8.5 letters indicating that the two drugs have similar efficacy [46]. Avastin was used to treat

Proliferative Diabetic Retinopathy (PDR) in a pilot study, and all 44/44 eyes treated with Avastin showed a decrease in vascular leakage a week after the intravitreal injection. However, neovascularization reoccurred in some patients after the injection as early as two weeks, showing that systemic side effects are likely and the need for frequent dosing to reduce the leakage [47]. As mentioned, Avastin has similar efficacy to Lucentis. The cost of 0.5 mg Lucentis vial is $1950, and the cost of 100 mg vial of Avastin is $550 [48]. Hence Avastin is used *off-label* as it is not approved by the FDA to treat wAMD [45].

2.4.1.4 Comparison between Eylea, Avastin, and Lucentis for the Treatment of Wet AMD

Two parallel Phase III clinical trials were conducted: VIEW 1 (the US and Canada) and VIEW 2 (Europe, Japan, Asia, and South America) to determine the clinical efficacy of Eylea and Lucentis to treat wAMD. Patients were randomized to three intravitreal injections of Eylea of 2 mg monthly, 2 mg every two months (after initial three-monthly doses), and 0.5 mg monthly. A fourth group received 0.5 mg of Lucentis monthly [49].
The primary endpoint of both VIEW 1 and VIEW 2 studies was to establish the non-inferiority of Eylea to Lucentis. It was determined that the proportion of patients who maintained their vision at 52 weeks lost <15 letters in both the studies. Patients receiving 2 mg of Eylea every two months maintained their vision at 52 weeks, reached 95.1% in VIEW1, and 95.6% in VIEW 2. In contrast, the patients receiving 0.5 mg Lucentis monthly who maintained their vision reached 95.9% in VIEW 1 and 96.3% in VIEW 2 studies. The results show that Eylea can be given once in two months as it has similar efficacy to Lucentis given monthly [49].

In a study by Klettner et al., Lucentis and Avastin were compared to study their ability to

neutralize VEGF in vitro. The study showed that Lucentis and Avastin have shown to neutralize VEGF in vitro when given at clinically appropriate doses. US FDA has thus approved Lucentis for the treatment of neovascular AMD [45]. Avastin and Lucentis are closely associated; the difference is at the fab region of Lucentis that varies by six amino-acids compared to Avastin [48]

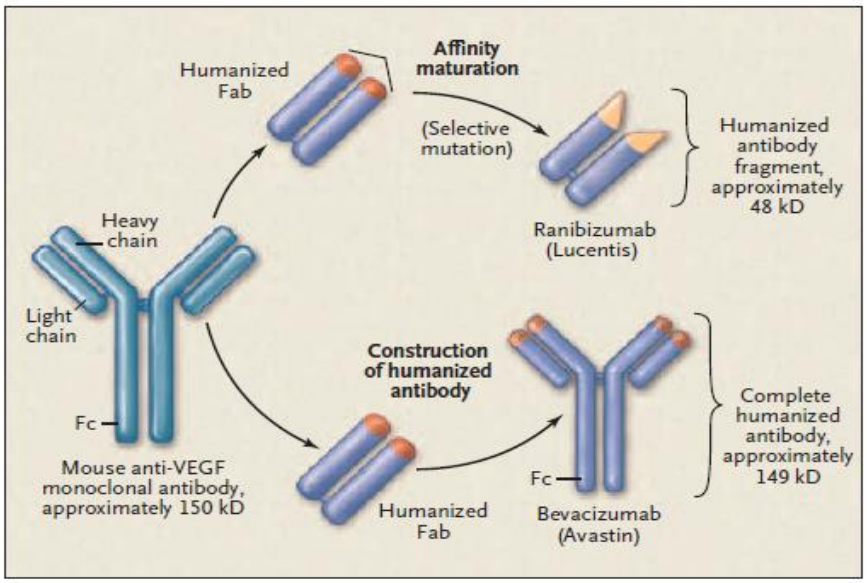

Figure 8: Relationship between Lucentis and Avastin [48].

2.4.1.5 Adverse effects of anti-VEGF agents and Conclusions:

Anti-VEGF agents have been effective in treating neovascular AMD. However, there are numerous side effects associated with the long-term use of anti-VEGF agents. VEGF is angiogenic, aids in neuroprotection, for example, increasing in vascular permeability, stimulating new blood vessels, and having a direct impact on neural cells [50]. VEGF is also implicated in the survival of photoreceptors and is vital for maintaining the health of the adult retina [38]. Therefore, the extended use of anti-VEGF agents has the potential to lead to undesired side-effects. The mode of delivery of these anti-VEGF agents is via injections directly into the

vitreous of the eye. Intravitreal injections are also associated with various side-effects like endophthalmitis and retinal detachment [38].

The most significant unmet need in ocular disease space is the demand for longer-acting therapeutics that can reduce the frequency of anti-VEGF injections by maintaining the therapeutic concentration of the drug in the vitreous. There is an opportunity to develop next-generation drugs that can be long-lasting and stabilize the vision of the elderly.

2.5 Polymeric Nanoparticles

In recent years nanoparticles have been explored as drug delivery modalities for ocular delivery because of their size, solubility, stability, and prolonged retention times. Numerous kinds of nanoparticles are used in ocular delivery, including chitosan, albumin, and poly(lactic-co-glycolic) acid [PLGA]. Nanoparticles are delivered through intravitreal injections directly into the vitreous chamber in the eye. Extensive research has shown that because of their small size, nanoparticles can bypass various ocular barriers and have been shown to maintain the required therapeutic concentration in the eye by maintaining drug retention at the site, thereby reducing the frequency of drug administration and increasing the time between the injections. Thus, nanoparticles have the exciting potential to provide a method of treating diseases of the anterior and posterior chamber of the eye.

2.5.1 Poly(lactic-co-glycolic) acid [PLGA] Nanoparticles

PLGA, poly-D, L-lactic-co-glycolic acid [51] has been extensively used for ocular delivery; it has been approved by the US FDA as a "clinically applicable material" as it is biocompatible, degradable, and non-toxic. PLGA can also be easily formulated with a variety of

drugs [6].

2.5.2 Properties of PLGA Nanoparticles

PLGA is formed by random ring-opening copolymerization of lactic acid and glycolic acid in the presence of a catalyst such as Tin(II) 2-ethyl hexanoate. The two distinct monomers, i.e., lactic acid and glycolic acid, are linked by the ester linkages resulting in the formation of PLGA[51]. The physicochemical characteristics of PLGA depend on several factors, including the molecular weight of PLGA, the ratio of lactide units to glycolide units (LA: GA), the size of the particles, the temperature at which the PLGA is stored, properties of the drug encapsulated inside the PLGA and the drug release conditions [52].

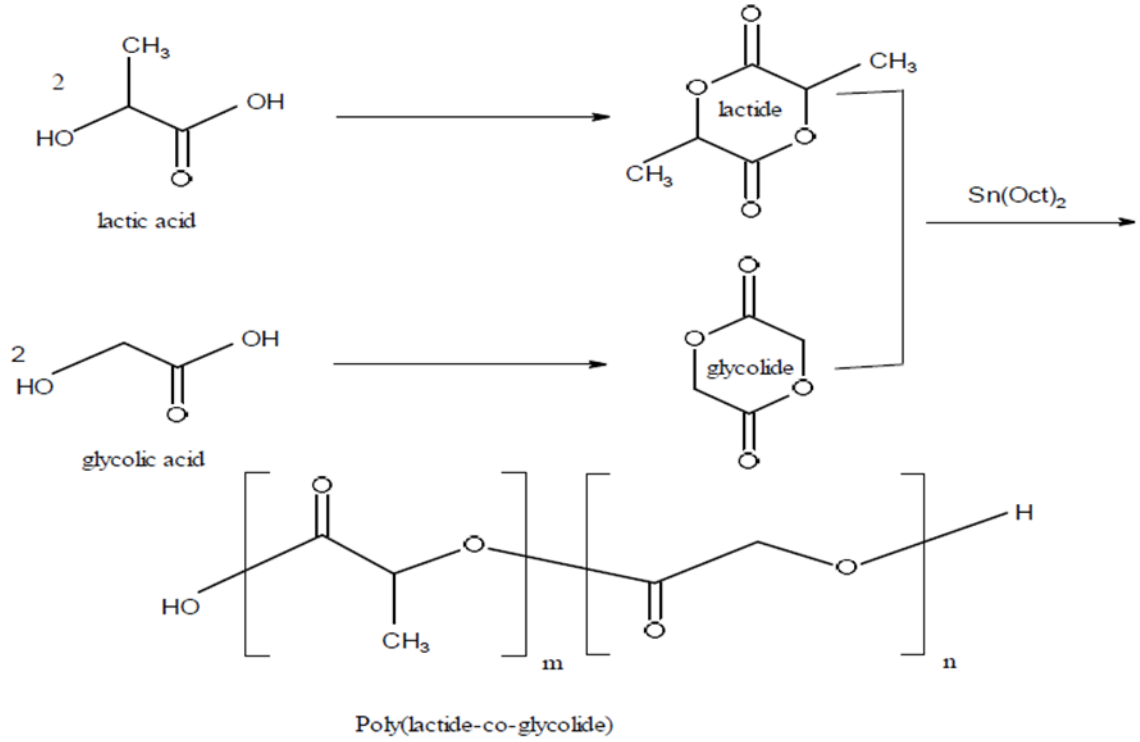

Figure 9: Poly lactic-co-glycolic acid (PLGA) synthesis from two distinct monomers – Lactic acid and Glycolic acid [53].

Various forms of PLGA can be obtained during the polymerization reaction by altering the ratio

of lactide units to glycolide units (L/G). The most significant factors responsible for the degradation rates and the drug release rates of PLGA are the molecular weight of PLGA and the degree of crystallization (ratio of L/G); these factors can change the rate of degradation of PLGA from weeks to months [8]. These properties of PLGA can be exploited to have sustained-release ocular delivery. PLGA with low molecular weight and high glycolic acid content degrades more rapidly due to the higher hydrophilicity of the glycolic acid due to the absence of the methyl side group and higher water uptake [54]. Lactic acid, on the other hand, is more hydrophobic and has lower water uptake leading to a slower degradation profile [51]. For example, PLGA 50:50 shows degradation over approximately 50-60 days [7]. The chirality of lactic acid also impacts degradation. For example, the poly-D, L-Lactic-co-Glycolic acid form of PLGA takes up to 12-16 months for complete biodegradation [7]. The degree of crystallinity of PLGA depends on the ratio of L/G, i.e., a decrease in lactic acid in the polymer results in a decrease in the crystallinity of the polymer. This can further influence the rate of drug release [54].

For a PLGA nanoparticle to be used as a drug delivery vehicle, several factors are needed to be considered, like the polydispersity index and the molecular weight of the polymer as it affects the degradation profile and hydrolysis of PLGA [55]. The hydrolysis of PLGA results in the formation of two distinct monomers – lactic acid and glycolic acid.

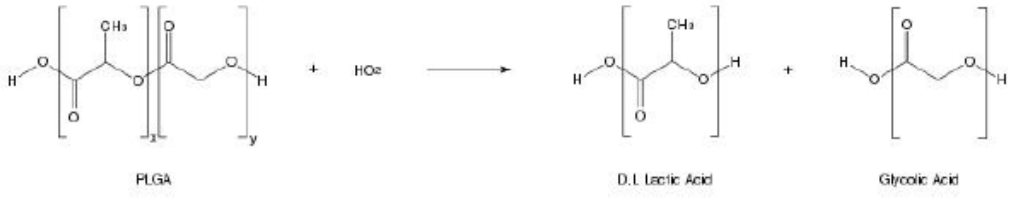

Figure 10: Hydrolysis of PLGA Nanoparticles [52].

PLGA is an attractive choice in drug delivery applications because the glass transition temperature (T_g) of PLGA is above physiological temperature, and, as a result, the polymer is glassy. The glassy structure of the PLGA results in the generation of a rigid chain structure, enhancing the mechanical strength of PLGA [55]. It has been shown that with a decrease in the molecular weight of the PLGA and the decrease in the Lactic acid units, the glass transition temperature (T_g) also decreases [52].

2.5.3 Fabrication techniques for PLGA Nanoparticles

There are numerous methods used to fabricate PLGA nanoparticles. The method of preparation plays a significant role in obtaining the desired functions. If the goal is to encapsulate drugs inside the PLGA nanoparticles, techniques including emulsification, nanoprecipitation methods, and salting-out processes can be used. For drug-loaded nanoparticles, the method selected is dependent on the drug release rate, the nature of the drug and the polymer to be used, and the disease to be targeted. The polymerization process, preformed polymers, and ionic gelation can also be used to make PLGA nanoparticles.

2.5.3.1 Preparation of PLGA Nanoparticles from Preformed Polymers or the Polymerization Process

The following techniques are used to fabricate the PLGA nanoparticles. However, PLGA nanoparticles are widely prepared from the preformed polymers [56].

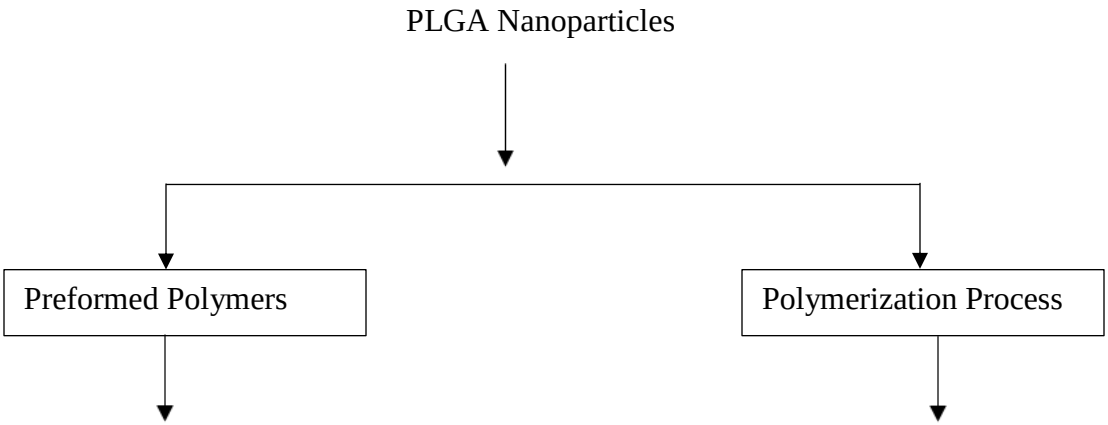

Solvent Evaporation	Emulsion
Nanoprecipitation	Mini Emulsion
Emulsification/Diffusion	Micro Emulsion
Salting Out	Interfacial Polymerization
Superficial Fluid Technology (SCF)	Radical Polymerization

Several factors govern the technique used to make the nanoparticles. The following factors are considered when choosing a specific technique for nanoparticle manufacturing: the use of less toxic reagents, the cost of the fabrication process, the % of the drug encapsulation efficiency, and the yield [56]. Drug release from the nanoparticles, both in vitro and in vivo, depends on multiple characteristics, including nanoparticle size, surface morphology, drug stability, drug encapsulation efficiency, degradation profile, thermodynamic properties, and the rate of diffusion [53]. These factors are directly influenced by the mode of nanoparticle preparation [7].

Table 1: Advantages and Disadvantages of different PLGA fabrication methods [54].

Advantages and drawbacks of techniques for PLGA particles preparation.

Method	Advantages	Drawbacks	Reference
Emulsification-solvent evaporation	Easy of scaling-up; Certain ability of controlling particle size;	Biomacromolecule instability at the interface or under shear stress; Batch-to-batch variance; Polydispersity of particle size.	[36,37]
Microfluidics	Precise of processing parameters; Monodispersity; Ease of fabricating double, triple and even higher order emulsions.	Instrument dependent; Relatively low yield.	[38,39]
Spray-drying	Fast and convenient; Suitable for industrial scaling-up; Less harsh conditions for proteins.	Adhesion of the MPs to the inner walls of the spray-dryer; Difficulty in control of size.	[27,40]
Phase separation	Tunable size with a wide range of processing parameters.	Negative effect of organic solvent on protein/nucleic acid function;	[27]
Nanoprecipitation	Ease of processing; Reproducibility.	Originally developed for hydrophobic drugs; Negative effect of organic solvent on protein/nucleic acid function.	[34,41]

The general overview of the different techniques used to make the PLGA nanoparticles is shown below.

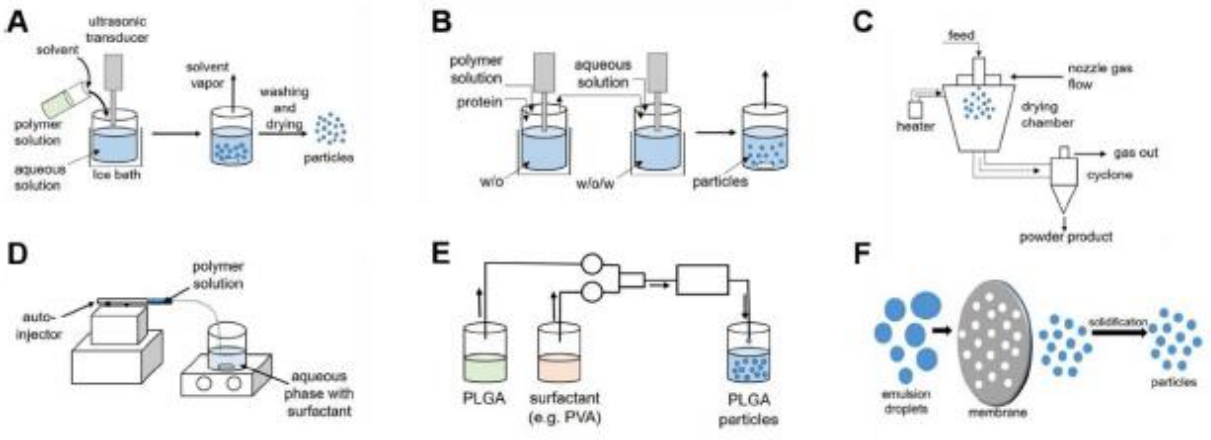

Figure 11: Different preparation techniques for PLGA Nanoparticles A. Single Emulsion Technique, B. Double Emulsion Method, C. Spray Drying, D. Nanoprecipitation, E. Microfluidics, and F. Membrane extrusion emulsification [57].

2.5.3.2 Biodegradation of PLGA and Drug Release Profile

The biodegradation of the PLGA determines the rate and mechanism of the drug release profile of the nanoparticles. PLGA generally shows a *biphasic drug release pattern.* Following an initial period of release that is primarily governed by diffusion of the drug and degradation of the polymer matrix. The degradation of the PLGA occurs mainly by bulk degradation via the cleavage of its backbone ester linkages by hydrolysis or biodegradation via chemical degradation first through the formation of oligomers and later into monomers [7]. However, the degradation of PLGA is a collaborative process of bulk degradation, bulk erosion, surface degradation, and surface erosion [52].

Nevertheless, the majority of PLGA biodegradation occurs by *Bulk Erosion* in which the PLGA polymers degrade uniformly throughout the entire bulk. It can also occur via *Surface Erosion* in which the degradation of the PLGA occurs layer-by-layer through the surface and gradually shrinking in size, as shown in the figure below:

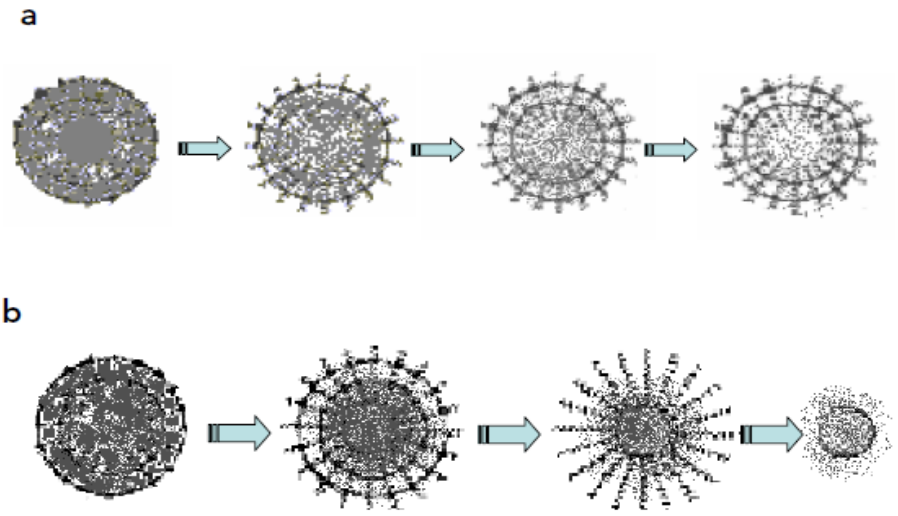

Figure 12: The degradation mechanism of the PLGA nanoparticles – a: Bulk Erosion and b: Surface Erosion [7].

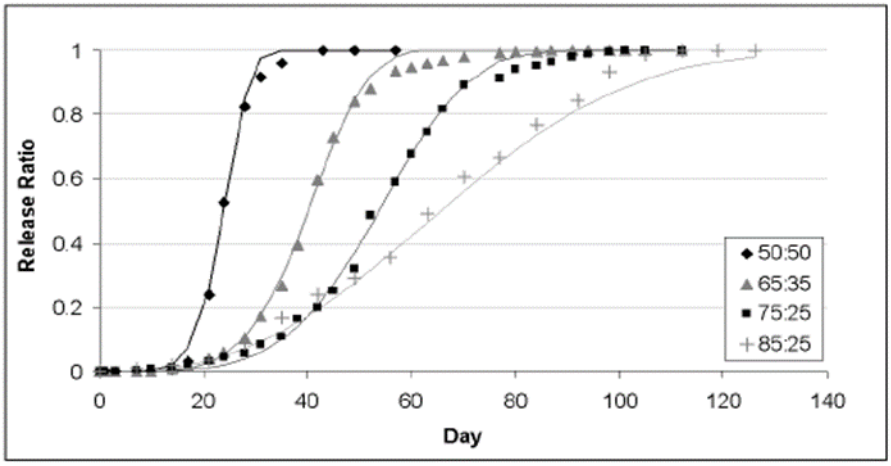

Figure 13: The rate of drug release from different types of PLGA by varying the ratio of L/G, ranging from weeks to months [52].

1. **PHASE I**

There are several factors responsible for the initial burst of drug release from the PLGA nanoparticles, including the type of the drug, concentration of the drug, and the hydrophobicity of the polymer matrix [51]. When PLGA nanoparticles encounter the release media, water penetrates inside the polymer matrix, and the drug is released rapidly as a function of solubility. Random scissions of the PLGA lower the molecular weight of the PLGA, but no monomers are formed in this phase [51].

2. **PHASE II**

The second phase of the PLGA drug release results in the depletion of the thicker drug layer resulting in continuous drug release. The water present inside the polymer matrix hydrolyzes the PLGA polymer into soluble oligomers and finally into monomers. The hydrolysis of PLGA creates a way for the drug to be released by erosion and diffusion until the complete

degradation of PLGA nanoparticles occurs [51].

PLGA has also been shown to have a *tri-phasic drug release pattern.* The initial phase results in a burst release of the drug and is often referred to as a burst phase. The second phase results in the formation of oligomers and monomers. If there is a drug remaining inside the PLGA, a significant condition occurs: the third and final phase, in which swelling of the PLGA nanoparticles occur and the drug gets released as the water-filled pores increase in size, ultimately destroying the PLGA [58].

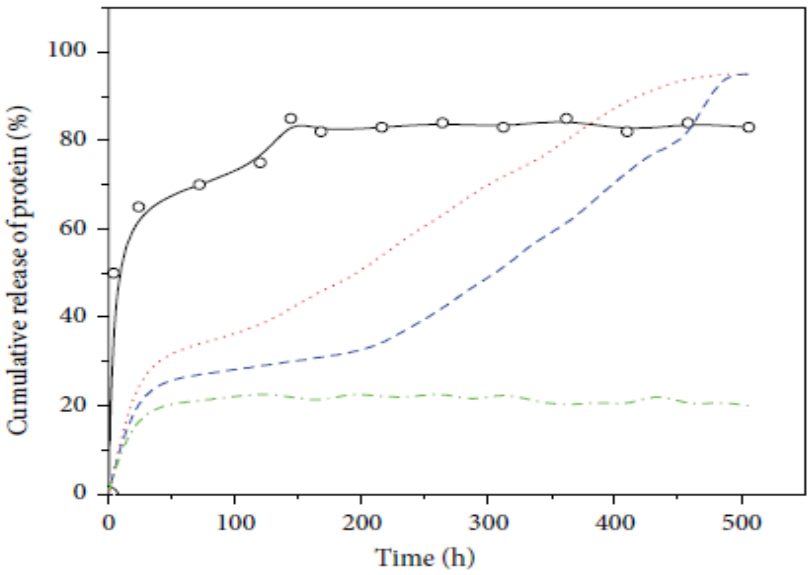

Figure 14: Drug release profiles of PLGA: Circle – BSA release from PLGA with the high initial burst, Red dotted lines – Biphasic Model, Blue dotted lines – Triphasic pattern and Green dotted lines – Incomplete release [59].

As mentioned earlier, PLGA nanoparticles degrade by hydrolytic cleavage of the backbone ester linkages into two distinct entities, i.e., lactic acid and glycolic acid. As both the lactic acid and glycolic acid are endogenous acid metabolites, the monomers enter the Krebs Cycle. They are quickly metabolized in the human body to H_2O and CO_2 [7], which are eliminated from the body through feces, respiration, and urine [8].

While the systemic toxicity of PLGA is relatively low as a result [60], it has been reported that the in-situ accumulation of the PLGA by-products, i.e., lactic acid and glycolic acid, during the degradation process, may result in increased local acidity that leads to irritation at the site of administration of PLGA [61].

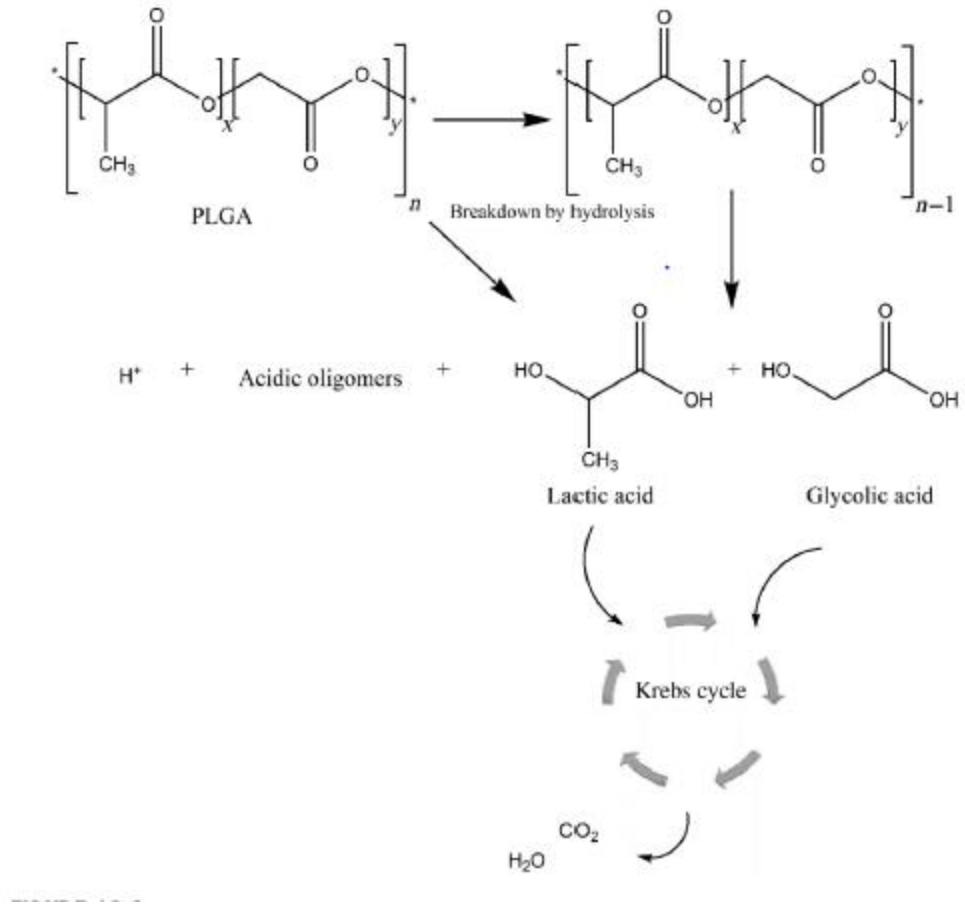

Figure 15: Hydrolysis of PLGA into endogenous acid metabolites and elimination from the body [60].

CHAPTER 3: MATERIALS AND METHODS

3.1 MATERIALS

Dichloromethane, polyvinyl alcohol [PVA 87-89% hydrolyzed, M_w= 31000-50000 and PVA 98% hydrolyzed, Mw =13000-23000], poly (lactic-co-glycolic) acid (PLGA) [50:50, M_w 24000-38000], and bovine serum albumin (BSA, Lyophilized powder, assay >= 98%) were purchased from Sigma Aldrich (Oakville, Ontario, Canada). Phosphate buffered saline solution (PBS, pH 7.4) was purchased from Bioshop (Burlington, Ontario, Canada). PLGA [PLGA 3:2, M_w = 10,000-15000] was purchased from Polyscitech (West Lafayette, IN). Purified water with a resistivity of 18.2 MΩ cm was prepared using a Millipore Barnstead water purification system (Graham, NC, USA). EZFlow 13 mm syringe filter with a 0.45 µm pore size was from Foxx Life Sciences (New Hampshire, United States) for Dynamic Light Scattering (DLS). Cellulose dialysis membranes with a molecular weight cutoff values of 1000 kD were purchased from Fisher Scientific (Massachusetts, United States). EZFlow 13 mm high-performance liquid chromatography (HPLC) grade syringe filters with a 0.22 µm pore size were purchased from Foxx Life Sciences (New Hampshire, United States), and an XBridge BEH200A SEC 3.5 µm 7.8 X 300 mm for HPLC was purchased from Waters (Mississauga, Ontario, Canada). PNIPAAM was synthesized in the Sheardown Lab at McMaster University, as previously described (Literature Review – In Situ Gelling Systems).

3.2 Synthesis of PLGA Nanoparticles

Optimization of PLGA nanoparticles was performed in order to obtain the highest drug encapsulation efficacy and desired particle size based on previous work from our lab.

PLGA was synthesized by the double emulsion method (W_1-O-W_2). In a typical double emulsion technique, BSA as a model for a protein drug of interest, was dissolved in 4.0 mL of PBS solution known as the inner aqueous phase (W_1). This drug solution was further added to PLGA 50:50 dissolved in 5.0 mL of dichloromethane, which acted as the oil (O) phase. A water in oil primary emulsion was created by ultrasonication using Misonix ultrasonic liquid processor (S-4000, Misonix, United States) at an intensity of 80% for two minutes.

Further emulsification was achieved by adding the primary emulsion to an outer aqueous phase that consisted of a stabilizer (i.e., PVA, 98% hydrolyzed, 0.083 mmol) dissolved in 74.7 mL of Millipore water (W_2) in a separate beaker. A water-oil-water emulsion was created by ultrasonication at an intensity of 90% for ten minutes. Therefore, homogenization is achieved in two steps resulting in the formation of double emulsion (W_1/O/W_2).

After the formation of double emulsion, the beaker was sealed with tin foil, and holes were created by the 18_G needle. The beaker was placed under constant magnetic stirring at 250 rpm for 48 h in the fume hood, such that evaporation of the oil phase (dichloromethane) occurred, resulting in hardened microspheres.

After 48 h of magnetic stirring, the nanoparticles were isolated using a Thermo scientific Sorvall WX90 ultracentrifuge (Fisher, United States) at 12000 rpm for 20 minutes at 24º C. After ultracentrifugation; the supernatant was collected for further analysis. The nanoparticles thus formed after ultracentrifugation were washed thrice with Milli-pore water and kept in the freezer for 24 h before freeze-drying. The nanoparticles were freeze-dried using a Freezone 2.5 Liter Benchtop Freeze dry system (Labconco, United States) and stored at 4º C until further use.

The synthesis protocol was optimized to obtain the highest drug encapsulation efficacy and particles of the desired particle size of 200-250 nm. Variables examined included intensity of sonication, speed of ultracentrifugation, composition, and amount of the stabilizer and PLGA nanoparticles. Four different batches of PLGA nanoparticles (Batch 1 – Batch 4) were prepared and characterized to assess encapsulation efficacy and particle size and compared with parameters for posterior segment ocular delivery.

3.2.1 Synthesis of PLGA Nanoparticles – Batch 1 and Batch 2

The following protocol was followed for PLGA Batch 1 and PLGA Batch 2:

Table 2: Synthesis of PLGA Nanoparticles – Batch 1 and Bath 2:

Synthesis of PLGA Nanoparticles – Batch 1 and Batch 2
1. **STEP 1**: **Formation of W_1/O Emulsion**: ➢ 0.04 g of BSA in 4 mL of PBS 2. **STEP 2**: **Oil Phase** ➢ 0.3 g of PLGA in 5 mL DCM 3. **STEP 3**: **Formation of W_1/O/W_2 Emulsion** ➢ 1.494 g of PVA in 74.7 mL H2O

For PLGA Batch 1 and PLGA Batch 2, different compositions of PLGA and PVA were used. The sonication intensity and the speed of ultracentrifugation were changed, and the amount of BSA was kept constant to determine the improved encapsulation efficacy and drug loading as shown:

Table 3: Compositions and synthesis conditions of PLGA nanoparticles:

PLGA NANOPARTICLES	BSA	PLGA	PVA	Ultracentrifugation
Batch 1	Lyophilized Powder, assay >= 98%	3:2 LA:GA, M_w = 10,000-15,000	87-89% hydrolyzed, M_w = 31000-50000	12,000 rpm for 20 minutes at 24˚C
Batch 2	Lyophilized Powder, assay >= 98%	50: 50 LA: GA, M_w = 24000-38000	98% hydrolyzed, M_w = 13000-23000	10,000 rpm for 15 minutes at 24˚C

The intensity of sonication was the following for Batch 1 and Batch 2:

Table 4: Ultrasonication conditions for PLGA Nanoparticles Batch 1

Sonicator	First Emulsion	Double Emulsion
Amplitude	50	90
Time	2 minutes	10 minutes
Energy	3376 J	21166 J

PLGA (3:2) encapsulated with BSA (drug) – **BATCH 1**

Table 5: Ultrasonication conditions for PLGA Nanoparticles Batch 2

Sonicator	First Emulsion	Double Emulsion
Amplitude	80	90

PLGA (50:50) encapsulated with BSA (drug) – **BATCH 2**

Time	2 minutes	10 minutes
Energy	2251 J	23910 J

Batch 2 of the PLGA Nanoparticle gave an improved encapsulation efficacy; therefore, PLGA 50:50 and PVA 98% were used to make Batch 3 and Batch 4 to obtain the highest encapsulation efficiency as shown:

3.2.2 PLGA Batch 3 and PLGA Batch 4

Table 6: Synthesis of PLGA Nanoparticles Batch 3 and Batch 4

PLGA Nanoparticles Batch 3	**PLGA Nanoparticles Batch 4**
STEP 1: **Formation of W1/O Emulsion**: ➢ **0.08 g** of BSA in 4 mL of PBS (Instead of **0.04 g** in Batch 1 and 2) **STEP 2**: **Oil Phase** ➢ 0.3 g of PLGA in 5 mL DCM **STEP 3**: **Formation of W1/O/W2 Emulsion** ➢ 1.494 g of PVA in 74.7 mL H2O	**STEP 1**: **Formation of W1/O Emulsion**: ➢ 0.04 g of BSA in 4 mL of PBS **STEP 2**: **Oil Phase** ➢ **0.6 g** of PLGA in 5 mL DCM (Instead of **0.3 g**) **STEP 3**: **Formation of W1/O/W2 Emulsion** ➢ 1.494 g of PVA in 74.7 mL H2O

The composition of BSA, PLGA, PVA, and intensity of sonication was kept constant for PLGA Batch 3 and Batch 4, and only the amount of BSA and PLGA were changed as shown in Table 6 and Table 7:

Table 7: Compositions and synthesis conditions of PLGA nanoparticles for Batch 3 and Batch 4:

PLGA NANOPARTICLES	BSA	PLGA	PVA
Batch 3 & Batch 4	Lyophilized Powder, assay >= 98%	50: 50 LA: GA, M_w = 24000-38000	98% hydrolyzed, M_w = 13000-23000

Table 8: Ultrasonication conditions for PLGA Nanoparticles Batch 3 and Batch 4

Sonicator	First Emulsion	Double Emulsion
Amplitude	80	90
Time	2 minutes	10 minutes

Intensity of Sonication for Batch 3 and Batch 4 for PLGA Nanoparticles

Four different batches of PLGA nanoparticles were synthesized, and encapsulation efficacy and drug loading are reported.

3.3 Nanoparticle Formation and Characterization

3.3.1 Nanoparticle Formation

Nanoparticles were formed by the double emulsion method (W1-O-W2). After freeze-drying, the PLGA nanoparticles were encapsulated with BSA resulting in hardened microspheres. The PLGA nanoparticles were optimized by following various protocols and formulations to obtain the highest % drug loading and required particle size. Particles prepared were characterized using a variety of techniques.

3.3.2 Dynamic Light Scattering (DLS)

The size of the PLGA nanoparticles was determined using a Brookhaven 90Plus particle analyzer running Particle Solutions Software (Version 2.6, Brookhaven Instruments Corporation, United States). It consists of 659 nm laser and a 90-degree detection angle. Samples containing the PLGA nanoparticles (10 mg) were appropriately diluted with PBS to get an acceptable level of transparency, and then the samples were filtered using a 0.45 µm filter. The DLS measurements were carried at 25º C. For each sample, five runs of five min each were performed. The size distribution and polydispersity are reported for different formulations of the PLGA nanoparticles.

3.3.3 Transmission Electron Microscopy (TEM)

TEM was used to determine the structure and shape of the PLGA nanoparticles. TEM images were obtained with a Jeol JEM-1200EX transmission electron microscope (Jeol USA) with an 80 kV electron beam. Samples were prepared by placing 4 µL of 10x diluted (in water) of particle solution on 200 mesh Formvar-coated copper grid to form a thinner layer, and a Kim wipe was used to gently blot the drop to form a thin film on a copper grid. The particles are air-dried on the grid overnight. The analysis was performed using a JEOL 1200EX TEMSCAN at a magnification of 5000.

3.3.4 Nanoparticle Tracking Analyzer (NTA)

Nanoparticle tracking analysis was used to calculate the size of the PLGA nanoparticles in real-time using 60 s recorded video images. Measurements were performed with a single nanoparticle tracking analysis Nanosight LM14 HS microscope (Malvern Panalytical,

Worcester, UK) equipped with a 532 nm laser, sCMOS camera, and NTA software 3.1. The NTA settings used for recording the video images for PLGA nanoparticles were: camera level = 8, shutter = 317, gain = 15, laser type = green, temperature = 24.1º C, viscosity = water (0.9 cp). Samples were prepared by re-dispersion of PLGA nanoparticles (100 µL) in PBS to get an acceptable level of transparency, and 1 mL of the sample was loaded onto the slide with a fixed stage using a 1 mL syringe until the sample reached the tip of the nozzle. The hydrodynamic radius of PLGA nanoparticles was tracked using an LM14 HS microscope in which light scattering allows the tracking of individual particles under Brownian Motion.

3.4 Drug Encapsulation Efficacy and % Drug Loading

The nanoparticles formed after the double emulsion method were centrifuged at 12000 rpm for 20 mins at 24ºC. After the ultracentrifugation, the supernatant was collected and analyzed for the presence of the drug, i.e., the BSA. The supernatant was filtered using a 0.22 µm nylon filter. The drug content in the supernatant was determined by analyzing the sample by high-performance liquid chromatography (HPLC) (Waters HPLC (2707 autosampler, 2489 UV spectrophotometer at an amplitude of 280 nm, 2475 Fluorescence detector at Excitation [λ_{ex} = 280 nm] and Emission [λ_{em} = 345 nm] 1525 binary HPLC pump, and Breeze 2 software). Analysis conditions included a 0.85 mL/min isocratic flow rate of buffer (1 L Milli Q water consisting of 2.47 g Sodium Phosphate Dibasic, Heptahydrate, 0.345 g Sodium Phosphate, Monobasic, Monohydrate, and 17.55 g NaCl) as the mobile phase using an XBridge BEH200A SEC column, a column temperature of 25º C and a partial loop injection volume of 27 µL max.

A standard calibration curve for BSA (25 – 400 µg/ml) was prepared and used to determine sample concentration. Encapsulation efficacy and Drug Loading were calculated using the following formulae:

$$\text{Encapsulation Efficacy} = \frac{\text{Amount of Drug Encapsulated}}{\text{The total amount of Drug Taken}} \text{ X } 100$$

$$\text{Drug Loading} = \frac{\text{Amount of Drug Encapsulated}}{\text{Total weight of Nanoparticles}} \text{ X } 100$$

UV spectroscopy was also used to determine the encapsulation efficacy and drug loading of the PLGA nanoparticles using a Beckman Instruments DU series 600 spectrophotometer. Phosphate Buffered Saline solution (PBS) was used as a control. 1 mL of the supernatant was collected after ultracentrifugation and was added in a transparent UV cuvette. Absorbance was measured at a wavelength (λ = 280 nm) to quantify the amount of BSA in the supernatant, and the reading was used to calculate the loading and encapsulation efficacy.

3.5 Drug Release Studies (PLGA-BSA)

In vitro drug release was performed in triplicate to study the release of BSA from the PLGA nanoparticles at 37º C. Dried PLGA nanoparticles (0.15 g) containing encapsulated BSA were suspended in a Falcon tube containing 10 mL PBS and kept in the shaker at 100 rpm at 37ºC. The tubes were periodically removed and centrifuged at 10,000 rpm for 5 min. Aliquots (1 mL) were removed at regular intervals and replaced with an equivalent volume of pre-warmed (37º C) PBS.

The supernatant was then collected, and the BSA content in the supernatant was analyzed using Waters HPLC (2707 autosampler, 2489 UV spectrophotometer at an amplitude of 280 nm,1525 binary HPLC pump, and Breeze 2 software) as described above.

3.6 Immobilization on PLGA Nanoparticles in PNIPAAM

The PLGA nanoparticles were prepared in a solution containing PNIPAAM [Poly(N-isopropylacrylamide)] to generate a nanoparticle-containing gel. For this process, 10 mg of the PLGA particles were added to 1 mL of PBS, and 150 mg of PNIPAAM (15%) was added to it and mixed properly. The PLGA-PNIPAAM-PBS mixture was transparent liquid at room temperature and formed a milky white, opaque gel at 37ºC. The gel thus formed was used for drug release studies.

3.7 In Vitro Drug Release– Free Drug (BSA)

Before performing the in vitro drug release studies, the release of BSA was conducted in a dialysis membrane to ensure that the membrane was permeable to the protein. For this study, 660 µg of BSA was dissolved in 1 mL of PBS and added into the dialysis membrane. The dialysis membrane was placed in a beaker with 10 mL of release media consisting of PBS. The same protocol was followed for the second beaker, and both beakers were placed in incubator and shaker at 37º C. The release of the free drug into the release media was studied. Samples were analyzed using a Waters HPLC, as described above.

3.8 Drug Release Studies

In vitro drug release studies were performed to assess the release kinetics of Bovine Serum Albumin (BSA) from nanoparticles. The drug-loaded nanoparticles were put into a cellulose dialysis membrane with a molecular weight cutoff values of 1000 kDa. Two different setups were performed for in vitro drug release studies.

1. **The release of BSA (drug) from PLGA Nanoparticles (PLGA-BSA) in a Static Incubator at 37º C**

The drug-loaded PLGA nanoparticles (10 mg) were dissolved in 1 mL PBS (PLGA-BSA) and were put into the dialysis membrane. The dialysis membrane was then placed in a sealed beaker containing 10 mL of PBS at a temperature of 37º C in a static incubator. The release of the BSA from the PLGA nanoparticles to the release media was evaluated. Aliquots (1 mL) were removed at regular intervals from the release media and replaced with an equivalent volume of pre-warmed (37º C) PBS and analyzed for BSA by HPLC.

2. **The release of BSA (drug) from PNIPAAM containing PLGA nanoparticles (PLGA-BSA-NIPAAM)**

The drug-loaded PLGA nanoparticles (10 mg) were dissolved in 1 mL PBS and then mixed with 150 mg of PNIPAAM (PLGA-BSA-PNIPAAM). The PNIPAAM containing the PLGA nanoparticles was put into a dialysis membrane. The dialysis membrane was then placed in a small beaker with 10 mL of PBS and maintained at a temperature of 37º C in a water bath with a speed of 30 rpm and shaken continuously. The release of the BSA from PLGA nanoparticles and then from the gelled scaffold (PNIPAAM) was studied and observed at regular intervals. Aliquots (1 mL) were removed and replaced with an equivalent volume of pre-warmed (37º C) PBS. Samples were analyzed using the same HPLC method as above.

CHAPTER 4: RESULTS AND DISCUSSION:

4.1 Synthesis of PLGA Nanoparticles

The PLGA nanoparticles (Batch 1 and Batch 2) were synthesized as described in section 3.2.1. Optimization of the protocol was performed in order to obtain the highest drug encapsulation efficacy and the desired particle size for posterior ocular delivery.

4.1.1 PLGA Batch 1 and PLGA Batch 2

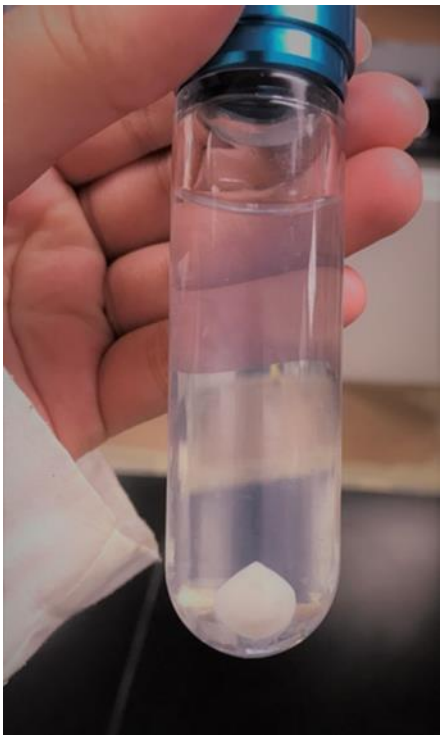

Figure 16: Batch 1: PLGA (3:2) after ultracentrifugation at 12000 rpm for 20 minutes at 24º C

Figure 17: Batch 2: PLGA (50:50) after ultracentrifugation at 10000 rpm for 15 minutes at 24º C

After the formation of the double emulsion, the nanoparticles were isolated by ultracentrifugation. PLGA Batch 1 and Batch 2 were ultracentrifuged, images of the

Nanoparticles are shown in Figure 16 and Figure 17. The nanoparticles settled at the bottom, and the supernatant is present above. The supernatant was further analyzed for the presence of the drug in order to determine the drug loading and the encapsulation efficiency.

After ultracentrifugation, the supernatant was collected to analyze for the presence of BSA by UV spectroscopy. The encapsulation efficacy and drug loading for the PLGA Batch 1 and PLGA Batch 2 are shown in Table 9, below. As noted, encapsulation efficiency ranged between 39 and 49%, with a drug loading of approximately 2% in both cases.

Table 9: Encapsulation Efficiency and Drug Loading for PLGA Batch 1 and PLGA Batch 2

PLGA Nanoparticles	**Encapsulation Efficiency (EE)** = (Amount of Drug Encapsulated/ Total amount of drug is taken)*100	**Drug Loading** = (Amount of Drug Encapsulated/Total weight of Nanoparticles)*100
Batch 1 (PLGA 3:2)	EE = **39.35%**	Drug Loading = **1.85%**
Batch 2 (PLGA 50:50)	EE = **49.17%**	Drug loading = **2.31%**

For PLGA Batch 1 and Batch 2, the composition of PLGA and PVA were changed while keeping the amount of BSA constant. The encapsulation efficiency ranged between 39% and 49% for PLGA Batch 1 and PLGA Batch 2, respectively. Research has shown that the processing parameters have a significant influence on the encapsulation efficiency of the PLGA nanoparticles. Low molecular weight PLGA (3:2) was used for Batch 1, and high molecular weight and equal ratio of lactide to glycolide (PLGA 50:50) was used for PLGA Batch 2. Thus,

Table 9 shows that encapsulation efficacy is highly influenced by the molecular weight of the PLGA and the hydrophilicity of the polymer, and the composition of the stabilizer [62]. The results obtained from Table 9 and the literature suggests that the encapsulation efficiency is greatly improved by using higher molecular weight PLGA due to lower chain mobility of the polymer as the drug (BSA) cannot diffuse out of the PLGA nanoparticles during the second emulsion, thereby increasing the encapsulation efficacy [63]. Thus, PLGA 50:50 was used to prepare PLGA Batch 3 and Batch 4 in attempts to obtain higher encapsulation efficacy.

4.1.2 PLGA Batch 3 and PLGA Batch 4

The PLGA nanoparticles (Batch 3 and Batch 4) were synthesized according to the methods described in Section 3.2.2. After the formation of double emulsion, the nanoparticles were ultracentrifuged at 10000 rpm for 30 minutes at 24º C for PLGA Batch 3, and at 12000 rpm for 20 minutes at 24º C for PLGA Batch 4. Digital images of PLGA Batch 3 and PLGA Batch 4 are shown in Figure 18 and Figure 19. It can be seen that the materials pelleted well with very little loss, as evidenced by the lack of cloudiness in the supernatant solution.

After ultracentrifugation, the supernatant was collected to analyze for the presence of BSA using UV spectroscopy to determine the encapsulation efficacy and drug loading of the PLGA nanoparticles. The encapsulation efficacy and drug loading for the PLGA Batch 3 and PLGA Batch 4 are shown in Table 10.

*Figure 18: BATCH 3**:** PLGA 50:50 with 0.08 g of BSA encapsulated and ultracentrifuged at 10,000 rpm for 30 minutes at 24º C*

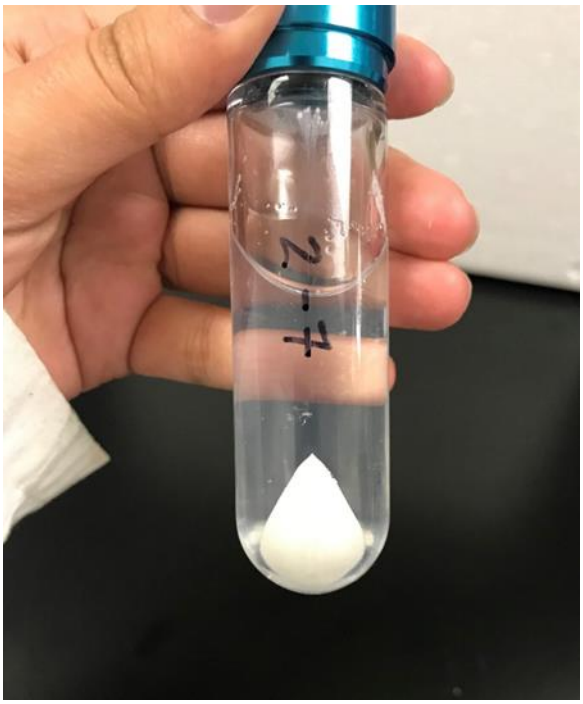

Figure 19: BATCH 4: PLGA 50:50 with 0.04 g of BSA encapsulated and ultracentrifuged at 12000 rpm for 20 minutes at 24º C

Table 10: Encapsulation Efficiency and Drug Loading for PLGA Batch 3 and PLGA Batch 4

PLGA Nanoparticles	**Encapsulation Efficiency (EE)** = (Amount of Drug Encapsulated/ Total amount of drug is taken)*100	**Drug Loading** = (Amount of Drug Encapsulated/Total weight of Nanoparticles)*100
Batch 3 (80 mg of BSA)	EE = **86.13%**	Drug Loading = **14.50%**
Batch 4 (600 mg of PLGA)	EE = **97.37%**	Drug loading = **2.43%**

As noted, the encapsulation efficiency of these materials is significantly higher than with the previous method used in the preparation of Batches 1 and 2. Furthermore, significantly higher drug loading was obtained for Batch 3 using this method. This is presumably due to the increase in the concentration of BSA (80 mg) that is doubled from the first two batches (40 mg). Research has shown that drug loading is affected by the concentration of the drug encapsulated and the concentration or molecular weight of the polymer [64]. The drug loading is also affected by the quantity and type of stabilizer [65].

The encapsulation efficacy was the highest for Batch 4 at 97%, as shown in Table 10 because the entrapment efficiency increases with an increase in the molecular weight and concentration of the PLGA (600 mg of PLGA) [62]. Therefore, by increasing the molecular weight and concentration of PLGA, high drug encapsulation efficacy of 97%, and drug loading of 2% was obtained.

A similar result was obtained using HPLC analysis of the supernatant, as summarized in Table 11.

Table 11: Encapsulation Efficiency of PLGA Batch 4 using HPLC Fluorescence

PLGA Nanoparticles	**Encapsulation Efficiency (EE)** = (Amount of Drug Encapsulated/ Total amount of drug is taken)*100
BATCH 4 (600 mg of PLGA) with HPLC Fluorescence	EE = **96.81%**

The Batch 4 PLGA nanoparticles, formed by Double Emulsion Method, showed the highest encapsulation efficacy. This protocol was therefore used for the preparation of all particles used for the assessment of drug release.

4.2 Nanoparticle Characterization

4.2.1 Dynamic Light Scattering (DLS)

The PLGA nanoparticles, prepared using the double emulsion method described in Section 3.2, were analyzed using DLS to determine the average effective diameter. The diameter, listed in Table 12, is in the range of 105.13 nm to 201.02 nm, and it indicates that the average diameter and polydispersity of the PLGA nanoparticles are influenced by the molecular weight and concentration of the PLGA [62]. This range of diameters for the nanoparticles is suitable for posterior ocular delivery as, at this size, they can cross the restrictive ocular barriers in the eye. Therefore, all of the formulations of the PLGA Nanoparticles meet the size objective.

Table 12: Average effective diameter and polydispersity of PLGA nanoparticles are shown. Four different batches of PLGA nanoparticles were synthesized containing various amounts and compositions of drug and polymer:

PLGA Nanoparticles	Effective Diameter (nm)	Polydispersity
BATCH 1 (PLGA 3:2)	105.13 nm	0.187
BATCH 2 (PLGA 50:50)	185.55 nm	0.206
BATCH 3 (PLGA 50:50 and 80 mg BSA)	111. 29 nm	0.202
BATCH 4 (PLGA 50:50 and 600 mg PLGA)	**201.02 nm**	**0.089**
CONTROL (PLGA 50:50, No BSA)	374.06 nm	0.349

The mean particle size of the PLGA nanoparticles can be changed by varying the processing parameters. The concentration of PLGA and the duration and intensity of sonication play a vital role in determining nanoparticle size [66]. The particle size varied from 100 nm to 200 nm, as seen in Table 12 by changing the concentrations of BSA, PVA, and PLGA [66], and the desired size can thus be obtained for posterior ocular delivery.

Although the size was slightly larger, the nanoparticles prepared in Batch 4 had the highest encapsulation efficacy and were therefore used for drug release studies and further nanoparticle characterization.

4.2.2 Transmission Electron Microscopy

The morphology of PLGA nanoparticles formed using the Double Emulsion Method described in section 3.3.3 based on the Batch 4 formulation (PLGA 50:50 with 600 mg of PLGA) can be observed in the TEM images shown in Figure 20.

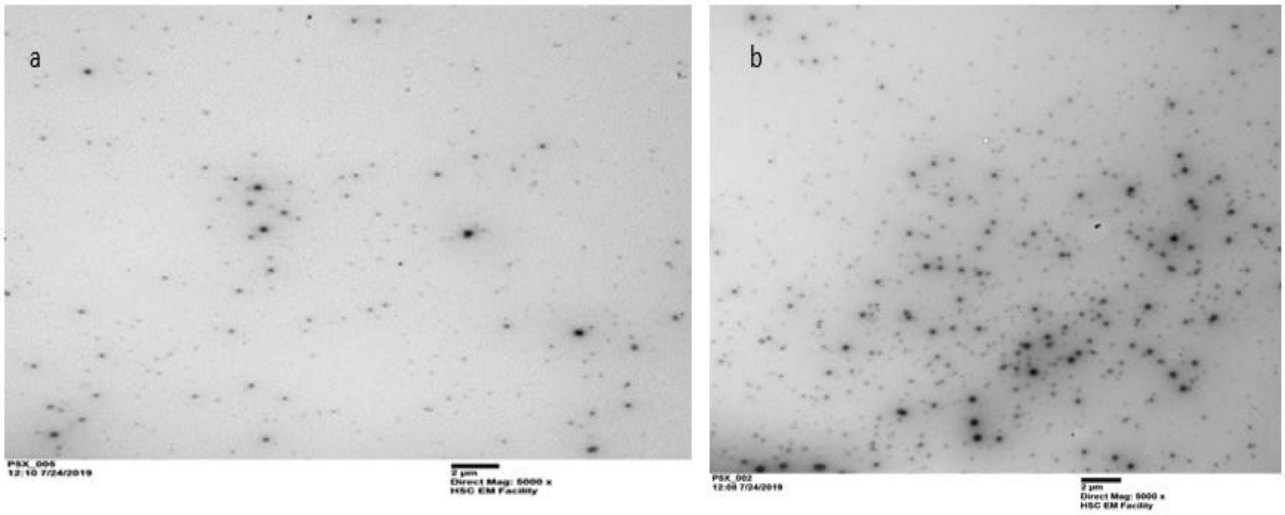

Figure 20: TEM images of PLGA nanoparticles prepared by Double Emulsion Method. The nanoparticles in the images were prepared according to the formulation listed in Table 4 for PLGA batch 4. The particles are air-dried overnight and after 24 hr observed under TEM. Magnification of the images is 5000 X.

The images show spherical, nano-sized PLGA nanoparticles that are relatively monodispersed were successfully synthesized.

4.2.3 Nanoparticle Tracking Analyzer (NTA)

The size of PLGA nanoparticles was measured using NTA to verify further that the nanoparticles are in the desired nano-size range for posterior ocular delivery. PLGA nanoparticles prepared using the double emulsion method with PLGA 50:50 and 600 mg of PLGA (Batch 4) were found to have a mean size of 254.6 nm.

Table 13: NTA Analysis of PLGA Nanoparticles

Sample	Mean	Mode	Standard Deviation
PLGA Nanoparticles	254.6 nm	178.2 nm	119.8 nm

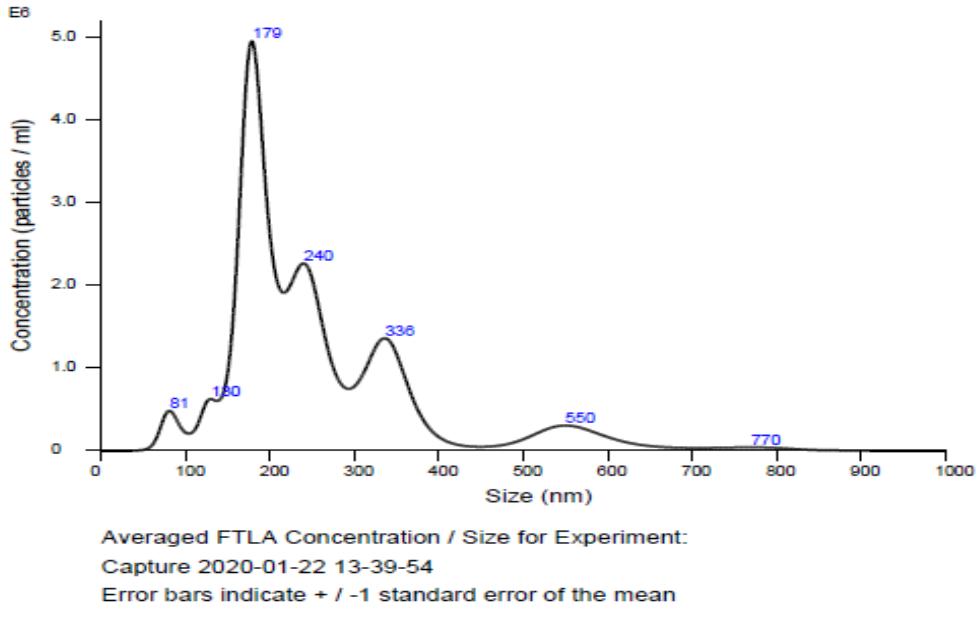

Figure 21: The size of PLGA Nanoparticles measured by NTA

The hydrodynamic radius of the PLGA nanoparticles was measured using both the DLS and NTA. Both the instruments showed similar sizing accuracy for the PLGA nanoparticles. The DLS showed a narrow size distribution, whereas the NTA gave individual particle sizing and mean effective diameter, similar to DLS. NTA was also used for sample visualization in real-time as the software produced a 60 s recorded video images of the PLGA nanoparticles as shown below [67].

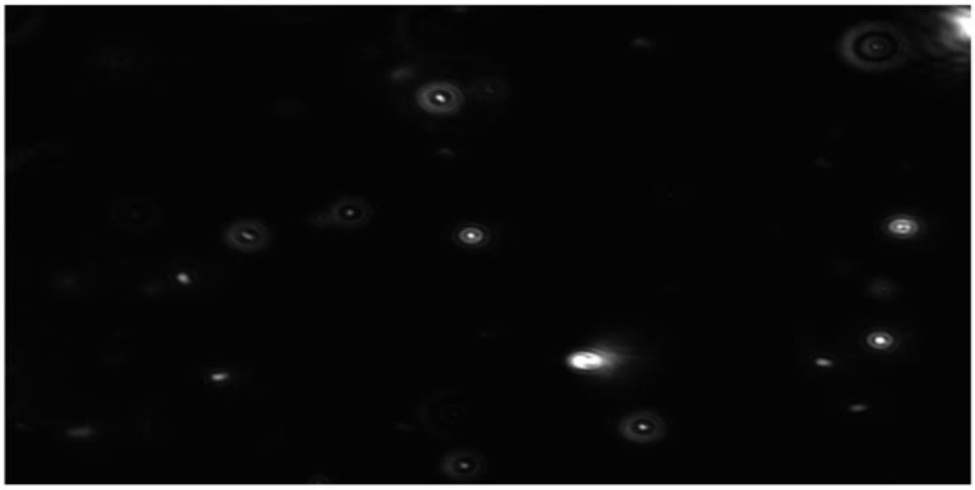

Figure 22: Screenshot of PLGA Nanoparticles moving in real time grabbed from the video generated by NTA software

4.3 Drug Release Studies (PLGA-BSA)

The release of BSA from PLGA nanoparticles using formulation Batch 4 from Table 12 was measured over seven days. Figure 23 shows the BSA release profile from PLGA nanoparticles.

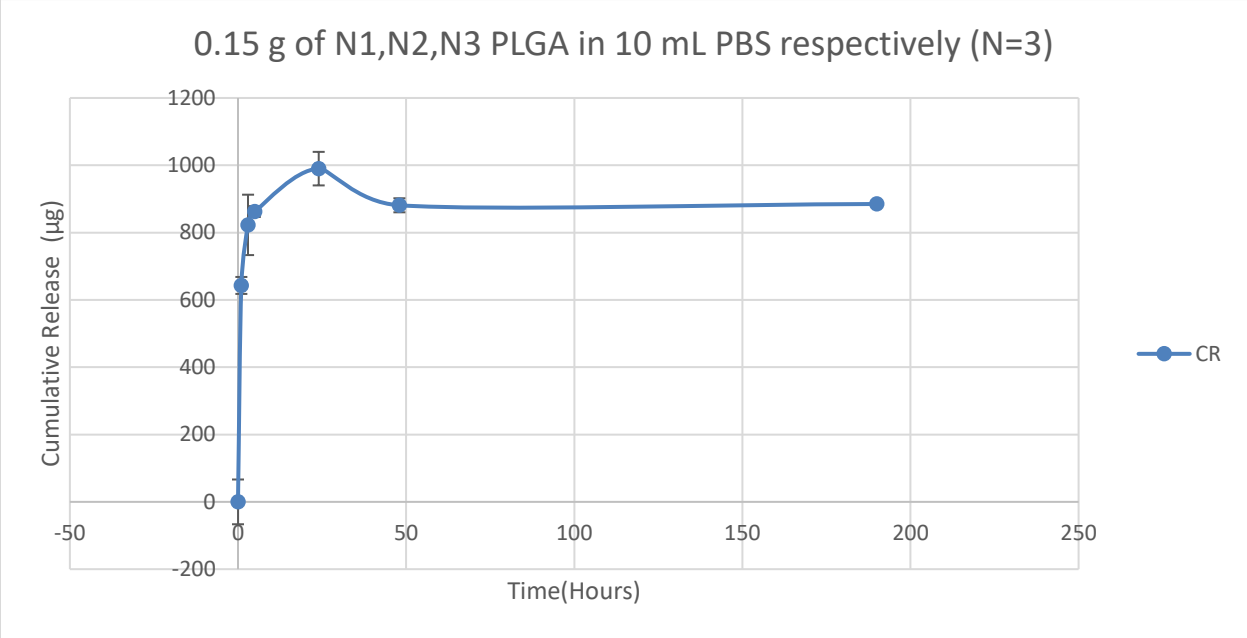

Figure 23: In-vitro release profile of BSA from PLGA Nanoparticles in the shaker at 100 rpm

According to the literature, the biodegradation of PLGA determines the rate and mechanism of drug release. This means that various phenomena, such as bulk erosion and polymer swelling, may be contributing to the release of the drug from the PLGA nanoparticles. In Figure 23, there is an initial burst release of BSA from PLGA nanoparticles; however, there is a decrease in the cumulative release after 24 h, and the total % BSA recovery in the release study was 31.49% due to BSA instability within PLGA nanoparticles.

There can be numerous factors responsible for the BSA instability within the PLGA nanoparticles as follows:

1. Dried PLGA microspheres (0.15 g) encapsulated with BSA (drug) were suspended in a falcon tube containing 10 mL PBS. Adsorption of protein (BSA) might have occurred in the falcon tube leading to protein losses. This could be mitigated by using a blocking buffer like Albumin or by using low binding tubes.

2. The degradation of PLGA nanoparticles results in acidic monomers, and this can result in acidic pH. As the degradation of PLGA nanoparticles proceeds, it causes BSA instability within PLGA. It was previously reported that the acidic denaturation of BSA leads to loss of the tertiary structure of the protein, thereby ultimately affecting the stability of BSA within PLGA nanoparticles [68]

To overcome the problems associated with the drug release, the following steps were considered to improve the drug release profile:

1. Mixing of the PLGA nanoparticles with a thermogelling scaffold developed in the Sheardown Lab – PNIPAAM for sustained drug release.

2. Drug release with PVA as a release media instead of PBS to make the nanoparticles more stable. PVA is extensively used as a stabilizer in Double Emulsion Method as it prevents the separation of the phases, making the nanoparticles more stable. Lamprecht et al. have shown that as the concentration of PVA increased, it resulted in a decrease in the coalescence of the PLGA nanoparticles making the emulsion droplets more stable [69]. However, this led to a sampling issue as both the polymer and the drug are big. (PLGA 50:50 – M_w = 24000-38000) and BSA (M_w = 66.5 kD_a).

3. Decrease the speed of ultracentrifugation (< 12000 rpm) as the possibility of PVA remaining in the supernatant and getting removed is high, making the nanoparticles unstable. However, this will result in loose particles, which will be challenging to isolate.

4. Change Recipe: Make particles more concentrated. However, in this case, an increase in PVA will impact the gelation of the PNIPAAM scaffold.

After considering all the above steps, mixing the PLGA nanoparticles with the thermogelling scaffold – PNIPAAM and releasing the drug from the gelled scaffold was considered the best alternative as it provides a potential avenue for sustained release of pharmaceuticals for the posterior segment of the eye through an injectable vehicle.

4.4 Incorporation of the PLGA Nanoparticles into Poly(N-isopropylacrylamide) [PNIPAAM]

The nanoparticles were incorporated into the PNIPAAM scaffold material as follows. The PNIPAAM is liquid at room temperature and forms a gel when heated above its lower critical solution temperature around 32º C. The PLGA-BSA-PNIPAAM is liquid at room and forms a gelled scaffold at 37º C, as shown in Figure 24.

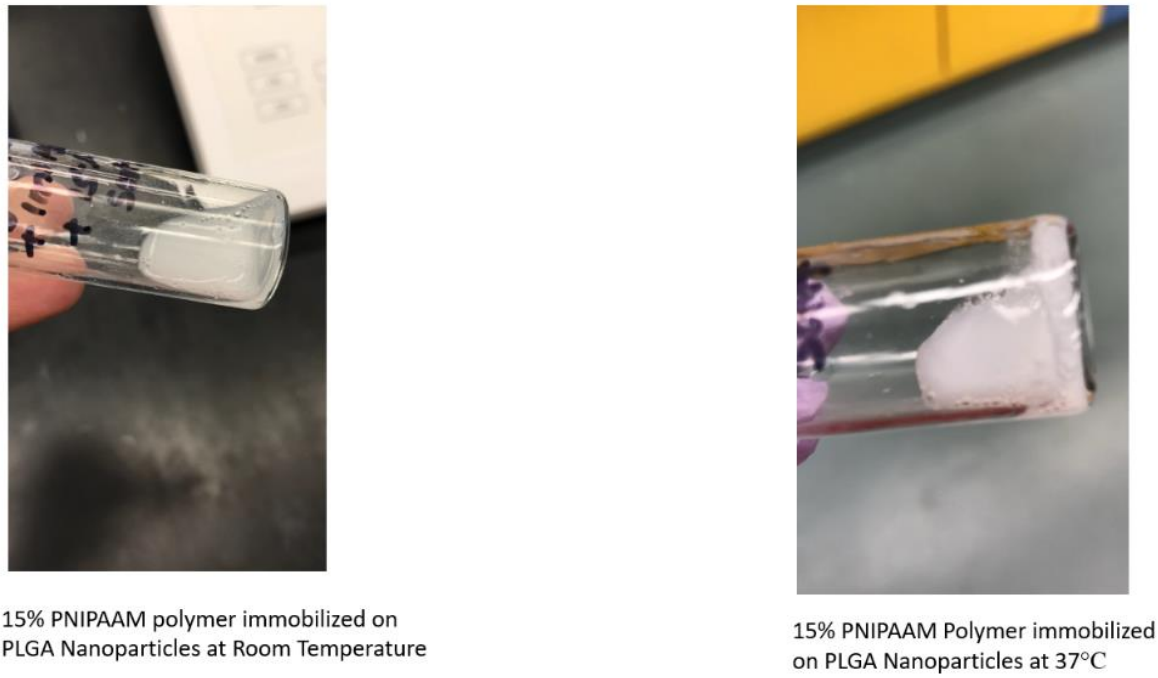

Figure 24: Screenshot of PNIPAAM polymer mixed with PLGA nanoparticles at room temperature(liquid) and at 37ºC (Gelled Scaffold) captured from the video

4.5 In-Vitro Drug Release- Free Drug (BSA)

The release of the BSA from the dialysis membrane was studied to determine if there is any obstacle to the passage of BSA from the dialysis membrane to the release media. The experiment setup was according to section 3.7.

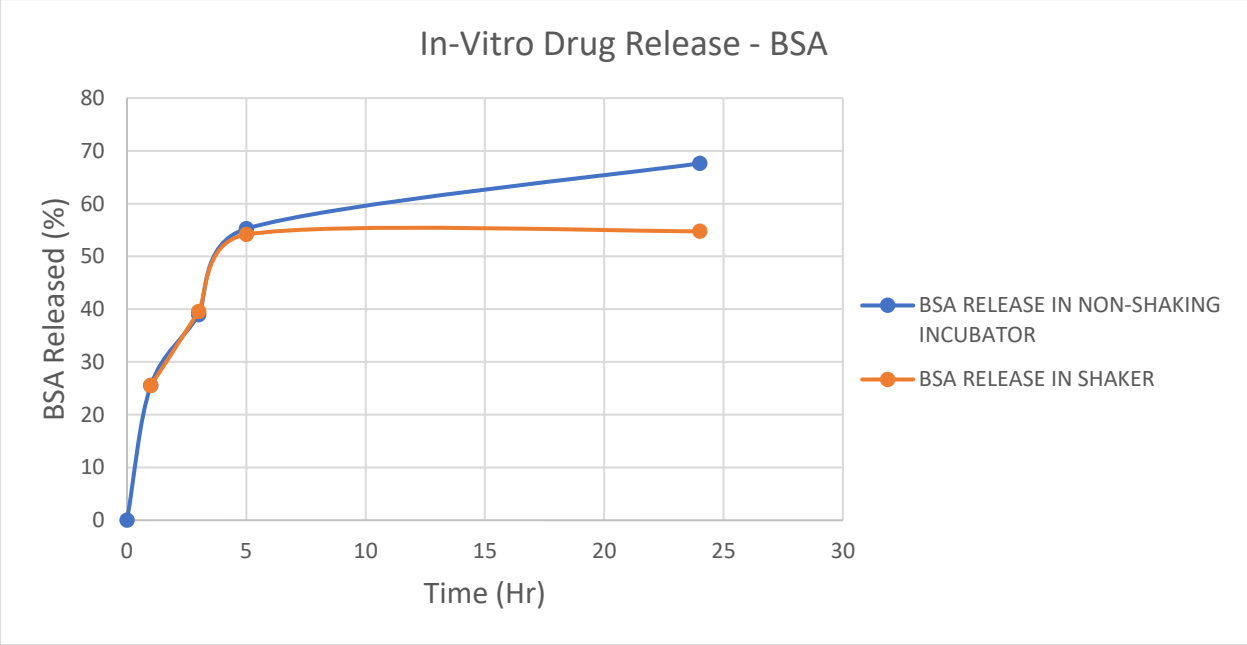

Figure 25: In-Vitro drug release – BSA from the dialysis membrane in Static Incubator and Shaker

The release of the free drug into the release medium was studied and observed under two conditions: 1. Static incubator at 37º C and 2. Shaker at 100 rpm at 37º C. Figure 25 shows that about 70% of the drug diffused to the release media within 24 hours in the non-shaking incubator compared to shaker in which 55% of the drug is released over 24 hours at 100 rpm. This indicates that BSA release from the dialysis membrane is sensitive to shaking at 100 rpm or

higher. However, it is clear that while the membrane does impede the passage of the BSA to some extent, diffusion through the membrane does occur.

4.6 Drug Release Studies

The drug release setup was according to section 3.8. Two experimental setups are conducted and studied: 1. The release of BSA from PLGA in a static incubator and 2. The release of BSA from PLGA and PNIPAAM in a water bath at 30 rpm. From the in-vitro study of free-BSA, it was found that the release of BSA from the dialysis membrane is sensitive to shaking, so for the experimental setup for the drug release of BSA from PLGA and PNIPAAM, a water bath was chosen at the speed of 30 rpm.

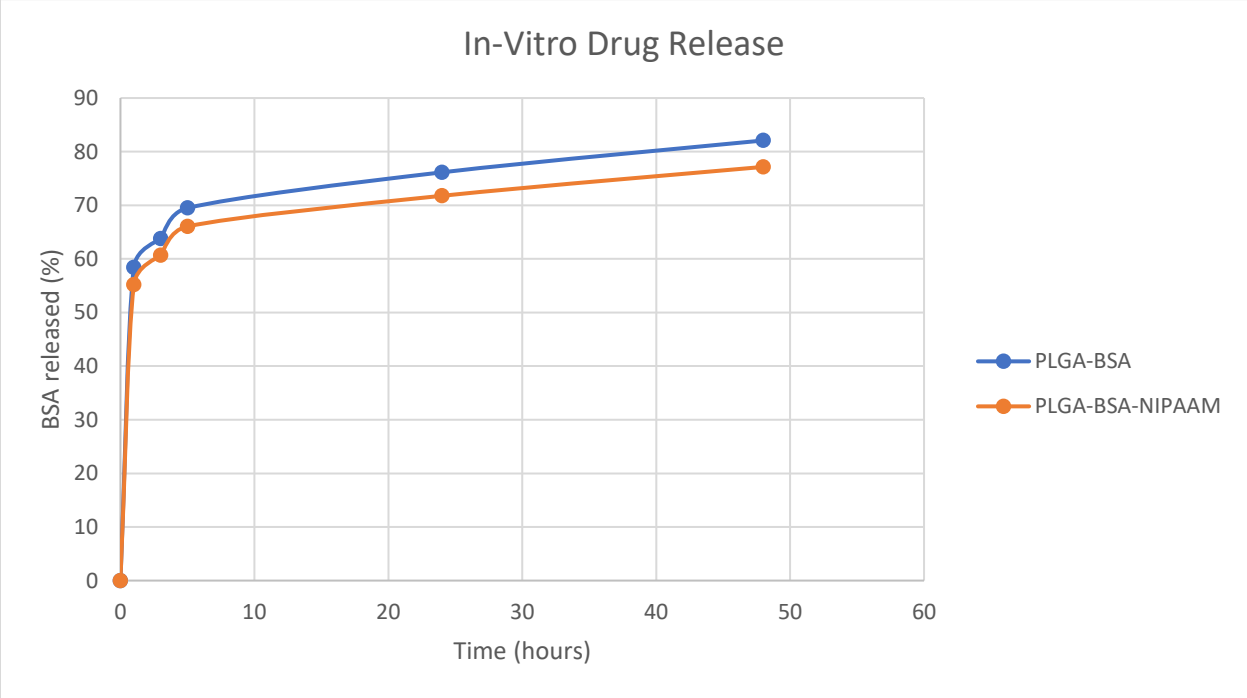

Figure 26: In-Vitro drug release of BSA from 1: PLGA-BSA in the static incubator at 37º C and 2: PLGA-BSA-PNIPAAM in the water bath at 30 rpm at 37º C.

Figure 26 shows that about 82% of the drug (BSA) diffused to the release media within 48 h from the PLGA nanoparticles in the static incubator in contrast to the release of BSA from the gelled scaffold - PLGA and PNIPAAM in which 77% of the drug is released over 48 h at 30 rpm. The similarity factor between the two curves is 69 (f2 = 69), which means that the two dissolution profiles are similar. The PNIPAAM was immobilized on the PLGA nanoparticles encapsulated with BSA to develop a slow-release formulation; however, the dissolution profiles are similar.

There can be various factors responsible for the similar dissolution profiles; however, the concentration of PNIPAAM (15%) may play the most significant role in the release of BSA from the gelled scaffold. At 15%, the PNIPAAM concentration may not be enough to sustain the release of the BSA from the gelled scaffold.

Future Steps:

1. Developing a slow-release formulation using 20% PNIPAAM instead of 15%. This is because as the concentration of PNIPAAM increases, the viscosity increases, and the gelled scaffold might hold the sustained release of the pharmaceuticals.
2. Use PLGA 80:20 because the increase in Lactic acid will increase the hydrophobicity of the polymer matrix and will degrade slowly over several months when compared to PLGA 50:50 that shows the fastest degradation profile.
3. Do the release of PLGA-BSA-NIPAAM in a static incubator instead of a water bath at 30 rpm as the BSA diffusion to the membrane is sensitive to shaking. The release can be done in the static incubator as the drug is for posterior ocular delivery.

CHAPTER 5: CONCLUSIONS

In conclusion, PLGA nanoparticles were synthesized for posterior ocular delivery. PLGA nanoparticles were synthesized by the double emulsion method (W_1-O-W_2). Spherical PLGA nanoparticles were produced as confirmed by TEM and NTA. DLS was used to confirm the size range of the different formulations of the PLGA nanoparticles. All of the PLGA nanoparticles were within the size range of 105.13 nm to 254.6 nm. Optimization of the experiments was performed, and modifications were made to the PLGA nanoparticle formulations to obtain the highest drug encapsulation efficacy and desired particle size range (< 300 nm) by changing the intensity of sonication, speed of ultracentrifugation, composition, and concentration of the stabilizer and PLGA nanoparticles, etc. Batch 4 of PLGA from Table 12 showed the highest encapsulation efficacy of 97.375% confirmed both by HPLC and UV spectrophotometer, and the particle size range confirmed by DLS was 201.02 nm. The size of the Batch 4 PLGA nanoparticles was further confirmed by TEM and NTA. The TEM images showed that the PLGA nanoparticles are relatively monodispersed with spherical morphologies. NTA indicated a mean size of 254.6 ±111.8 nm, and the video of the PLGA nanoparticles was generated moving in real-time indicated spherical morphology. As the Batch 4 of PLGA nanoparticles had the highest encapsulation efficacy and desired size, the formulation was chosen for drug release studies.

Based on the in vitro drug release – PLGA-BSA, the total % BSA recovery in the release study was 31.49% due to the BSA instability within the PLGA nanoparticles, and there can be numerous factors responsible for it, as mentioned. The drug release suggested the need to use a

dialysis membrane for the release of BSA from the PLGA nanoparticles. Therefore, the PLGA nanoparticles were mixed with a thermogelling scaffold - PNIPAAM developed in the Sheardown Lab, such that a slow-release formulation can be developed. At 37º C, it formed a gelled scaffold. In vitro drug release studies were performed to assess the release kinetics of Bovine Serum Albumin (BSA) from nanoparticles incorporated into the scaffold. The drug-loaded nanoparticles were put into a cellulose dialysis membrane with a molecular weight cutoff values of 1000 kDa. Two different setups were performed for in vitro drug release studies: PLGA-BSA in the static incubator and PLGA-BSA-NIPAAM in the water bath at 30 rpm. The study showed that 82% of the drug (BSA) diffused to the release media from PLGA-BSA within 48 h when compared to 77% of the drug (BSA) diffused to the release media from the gelled scaffold of PLGA-BSA-NIPAAM within 48 h. Overall, the results suggest that these nanoparticles (PLGA-BSA and PLGA-BSA-PNIPAAM) have the potential for further development as drug delivery modalities for posterior segment ocular delivery.

Future experiments should be focused on developing a slow-release formulation using a higher concentration of PNIPAAM to sustain the release of BSA from the PLGA nanoparticles and the in vitro release of BSA from the gelled PLGA-BSA-PNIPAAM scaffold should be done using a dialysis membrane, and the samples should be analyzed by using HPLC (UV Spectrophotometer and Fluorescence) and compared with PLGA-BSA to study and compare the drug release rate. Additionally, an in vitro release study of IgG from PLGA-IgG-PNIPAAM can be done using a similar method stated for the release of BSA from HPLC fluorescence to compare the proteins.

CHAPTER 6

[1] E. M. del Amo and A. Urtti, “Current and future ophthalmic drug delivery systems. A shift to the posterior segment,” *Drug Discov. Today*, vol. 13, no. 3–4, pp. 135–143, 2008.

[2] R. Gaudana, J. Jwala, S. H. S. Boddu, and A. K. Mitra, “Recent perspectives in ocular drug delivery,” *Pharm. Res.*, vol. 26, no. 5, pp. 1197–1216, 2009.

[3] S. H. Kim, K. G. Csaky, N. S. Wang, and R. J. Lutz, “Drug elimination kinetics following subconjunctival injection using dynamic contrast-enhanced magnetic resonance imaging,” *Pharm. Res.*, vol. 25, no. 3, pp. 512–520, 2008.

[4] U. B. Kompella, A. C. Amrite, R. Pacha Ravi, and S. A. Durazo, “Nanomedicines for back of the eye drug delivery, gene delivery, and imaging,” *Prog. Retin. Eye Res.*, vol. 36, pp. 172–198, 2013.

[5] D. Ghate and H. F. Edelhauser, “Ocular drug delivery,” *Expert Opin. Drug Deliv.*, vol. 3, no. 2, pp. 275–287, 2006.

[6] H. H. Shen *et al.*, “Nanocarriers for treatment of ocular neovascularization in the back of the eye: New vehicles for ophthalmic drug delivery,” *Nanomedicine*, vol. 10, no. 13, pp. 2093–2107, 2015.

[7] I. Bala, S. Hariharan, and M. N. V. R. Kumar, “PLGA nanoparticles in drug delivery: The state of the art,” *Crit. Rev. Ther. Drug Carrier Syst.*, vol. 21, no. 5, pp. 387–422, 2004.

[8] E. M. Elmowafy, M. Tiboni, and M. E. Soliman, *Biocompatibility , biodegradation and biomedical applications of poly (lactic acid)/ poly (lactic - co - glycolic acid) micro and nanoparticles*, vol. 49, no. 4. Springer Singapore, 2019.

[9] D. Thassu and G. J. Chader, *Ocular drug delivery systems: Barriers and application of nanoparticulate systems*. 2012.

[10] A. Urtti, “Challenges and obstacles of ocular pharmacokinetics and drug delivery,” *Adv. Drug Deliv. Rev.*, vol. 58, no. 11, pp. 1131–1135, 2006.

[11] A. Farkouh, P. Frigo, and M. Czejka, “Systemic side effects of eye drops: A pharmacokinetic perspective,” *Clin. Ophthalmol.*, vol. 10, pp. 2433–2441, 2016.

[12] A. Mandal, R. Bisht, I. D. Rupenthal, and A. K. Mitra, “Polymeric micelles for ocular drug delivery: From structural frameworks to recent preclinical studies,” *J. Control. Release*, vol. 248, pp. 96–116, 2017.

[13] D. Psimadas, P. Georgoulias, V. Valotassiou, and G. Loudos, “Molecular Nanomedicine Towards Cancer :,” *J. Pharm. Sci.*, vol. 101, no. 7, pp. 2271–2280, 2012.

[14] S. J. Smith, B. D. Smith, and B. G. Mohney, “Ocular side effects following intravitreal injection therapy for retinoblastoma: A systematic review,” *Br. J. Ophthalmol.*, vol. 98, no. 3, pp. 292–297, 2014.

[15] G. D. Novack, “Ophthalmic drug delivery: Development and regulatory considerations,” *Clin. Pharmacol. Ther.*, vol. 85, no. 5, pp. 539–543, 2009.

[16] I. A. El-Ghrably, A. Saad, and C. Dinah, “A Novel Technique for Repositioning of a Migrated ILUVIEN® (Fluocinolone Acetonide) Implant into the Anterior Chamber,” *Ophthalmol. Ther.*, vol.

4, no. 2, pp. 129–133, 2015.

[17] A. A. Moshfeghi and G. A. Peyman, “Micro- and nanoparticulates B,” vol. 57, pp. 2047–2052, 2005.

[18] S. Zhang and H. Uluda, “Expert Review Nanoparticulate Systems for Growth Factor Delivery,” vol. 26, no. 7, 2009.

[19] J. M. Anderson and M. S. Shive, “Biodegradation and biocompatibility of PLA and PLGA microspheres ☆,” *Adv. Drug Deliv. Rev.*, vol. 64, pp. 72–82, 2012.

[20] J. Hsu, “Drug delivery methods for posterior segment disease,” pp. 235–239, 2007.

[21] W. H. De Jong, “Drug delivery and nanoparticles : Applications and hazards,” vol. 3, no. 2, pp. 133–149, 2008.

[22] E. Eljarrat-Binstock, F. Raiskup, J. Frucht-Pery, and A. J. Domb, “Transcorneal and transscleral iontophoresis of dexamethasone phosphate using drug loaded hydrogel,” *J. Control. Release*, vol. 106, no. 3, pp. 386–390, 2005.

[23] S. D. Fitzpatrick, M. A. Jafar Mazumder, B. Muirhead, and H. Sheardown, “Development of injectable, resorbable drug-releasing copolymer scaffolds for minimally invasive sustained ophthalmic therapeutics,” *Acta Biomater.*, vol. 8, no. 7, pp. 2517–2528, 2012.

[24] J. Zhang *et al.*, “An Injectable Hydrogel Prepared Using a PEG/Vitamin E Copolymer Facilitating Aqueous-Driven Gelation,” *Biomacromolecules*, vol. 17, no. 11, pp. 3648–3658, 2016.

[25] L. A. Wells, S. Furukawa, and H. Sheardown, “Photoresponsive PEG-anthracene grafted hyaluronan as a controlled-delivery biomaterial,” *Biomacromolecules*, vol. 12, no. 4, pp. 923–932, 2011.

[26] N. Kunou *et al.*, “Long-term sustained release of ganciclovir from biodegradable scleral implant for the treatment of cytomegalovirus retinitis,” *J. Control. Release*, vol. 68, no. 2, pp. 263–271, 2000.

[27] E. Dejuan *et al.*, “(12) United States Patent,” vol. 2, no. 12, 2012.

[28] R. Lo, P. Y. Li, S. Saati, R. N. Agrawal, M. S. Humayun, and E. Meng, “A passive MEMS drug delivery pump for treatment of ocular diseases,” *Biomed. Microdevices*, vol. 11, no. 5, pp. 959–970, 2009.

[29] J. Jiang, J. S. Moore, H. F. Edelhauser, and M. R. Prausnitz, “Intrascleral Drug Delivery to the Eye Using Hollow Microneedles,” *Pharm. Res.*, vol. 26, no. 2, pp. 395–403, 2009.

[30] L. S. Lim, P. Mitchell, J. M. Seddon, F. G. Holz, and T. Y. Wong, “Age-related macular degeneration.,” *Lancet (London, England)*, vol. 379, no. 9827, pp. 1728–38, 2012.

[31] R. Guymer, P. Luthert, and A. Bird, “Changes in Bruch’s membrane and related structures with age,” *Prog. Retin. Eye Res.*, vol. 18, no. 1, pp. 59–90, 1999.

[32] F. G. Holz, S. Schmitz-Valckenberg, and M. Fleckenstein, “Recent developments in the treatment of age-related macular degeneration,” *J. Clin. Invest.*, vol. 124, no. 4, pp. 1430–1438, 2014.

[33] S. Iyer, A. E. Radwan, A. Hafezi-Moghadam, P. Malyala, and M. Amiji, “Long-acting intraocular Delivery strategies for biological therapy of age-related macular degeneration,” *J. Control.*

Release, vol. 296, no. January, pp. 140–149, 2019.

[34] J. Tuo, C. M. Bojanowski, and C. C. Chan, "Genetic factors of age-related macular degeneration," *Prog. Retin. Eye Res.*, vol. 23, no. 2, pp. 229–249, 2004.

[35] S. B. Bressler, "Introduction: Understanding the Role of Angiogenesis and Antiangiogenic Agents in Age-Related Macular Degeneration," *Ophthalmology*, vol. 116, no. 10 SUPPL., pp. S1–S7, 2009.

[36] M. Saint-Geniez *et al.*, "Endogenous VEGF is required for visual function: Evidence for a survival role on Müller cells and photoreceptors," *PLoS One*, vol. 3, no. 11, 2008.

[37] T. A. Ciulla and P. J. Rosenfeld, "Anti-vascular endothelial growth factor therapy for neovascular ocular diseases other than age-related macular degeneration," *Curr. Opin. Ophthalmol.*, vol. 20, no. 3, pp. 166–174, 2009.

[38] M. S. R. Jardeleza and J. W. Miller, "Review of anti-vEGF therapy in proliferative diabetic retinopathy," *Semin. Ophthalmol.*, vol. 24, no. 2, pp. 87–92, 2009.

[39] J. Hainsworth *et al.*, "new england journal," pp. 2335–2342, 2020.

[40] M. Ohr and P. K. Kaiser, "Intravitreal aflibercept injection for neovascular (wet) age-related macular degeneration," *Expert Opin. Pharmacother.*, vol. 13, no. 4, pp. 585–591, 2012.

[41] G. M. Keating, "Aflibercept: A Review of Its Use in Diabetic Macular Oedema," *Drugs*, vol. 75, no. 10, pp. 1153–1160, 2015.

[42] F. Semeraro, F. Morescalchi, S. Duse, F. Parmeggiani, E. Gambicorti, and C. Costagliola, "Aflibercept in wet AMD: Specific role and optimal use," *Drug Des. Devel. Ther.*, vol. 7, pp. 711–722, 2013.

[43] M. R. Barakat and P. K. Kaiser, "VEGF inhibitors for the treatment of neovascular age-related macular degeneration," *Expert Opin. Investig. Drugs*, vol. 18, no. 5, pp. 637–646, 2009.

[44] P. Zeitler;, K. Hirst;, L. Pyle, and B. Linder, "New England Journal (332-342).pdf," *N. Engl. J. Med.*, vol. 366, pp. 2247–2256, 2012.

[45] A. Klettner and J. Roider, "Comparison of bevacizumab, ranibizumab, and pegaptanib in vitro: Efficiency and possible additional pathways," *Investig. Ophthalmol. Vis. Sci.*, vol. 49, no. 10, pp. 4523–4527, 2008.

[46] K. F. Adams, "New England Journal Medicine," *N. Engl. J. Med.*, vol. 360, no. 25, pp. 2605–2615, 2009.

[47] R. L. Avery, J. Pearlman, D. J. Pieramici, and M. D. Rabena, "in the Treatment of Proliferative Diabetic Retinopathy," no. January, 2006.

[48] R. Steinbrook, "and the Treatment of Macular Degeneration," pp. 1409–1412, 2020.

[49] J. S. Heier *et al.*, "Intravitreal aflibercept (VEGF trap-eye) in wet age-related macular degeneration," *Ophthalmology*, vol. 119, no. 12, pp. 2537–2548, 2012.

[50] E. Storkebaum, D. Lambrechts, and P. Carmeliet, "VEGF: Once regarded as a specific angiogenic factor, now implicated in neuroprotection," *BioEssays*, vol. 26, no. 9, pp. 943–954, 2004.

[51] S. Sharma, A. Parmar, S. Kori, and R. Sandhir, "PLGA-based nanoparticles: A new paradigm in

biomedical applications," *TrAC - Trends Anal. Chem.*, vol. 80, pp. 30–40, 2016.

[52] H. K. Makadia, S. J. Siegel, and A. Krackow, "Poly Lactic-co-Glycolic Acid (PLGA) as biodegradable controlled drug delivery carrier," *Polymers (Basel).*, vol. 3, no. 3, pp. 1377–1397, 2011.

[53] R. H. Ansary, M. B. Awang, and M. M. Rahman, "Biodegradable poly(D,L-lactic-co-glycolic acid)-based micro/nanoparticles for sustained release of protein drugs - A review," *Trop. J. Pharm. Res.*, vol. 13, no. 7, pp. 1179–1190, 2014.

[54] D. Ding and Q. Zhu, "Recent advances of PLGA micro/nanoparticles for the delivery of biomacromolecular therapeutics," *Mater. Sci. Eng. C*, vol. 92, no. January, pp. 1041–1060, 2018.

[55] R. A. Jain, "The manufacturing techniques of various drug loaded biodegradable poly(lactide-co-glycolide) (PLGA) devices," *Biomaterials*, vol. 21, no. 23, pp. 2475–2490, 2000.

[56] B. V. N. Nagavarma, H. K. S. Yadav, A. Ayaz, L. S. Vasudha, and H. G. Shivakumar, "Different techniques for preparation of polymeric nanoparticles- A review," *Asian J. Pharm. Clin. Res.*, vol. 5, no. SUPPL. 3, pp. 16–23, 2012.

[57] E. Swider, O. Koshkina, J. Tel, L. J. Cruz, I. J. M. de Vries, and M. Srinivas, "Customizing poly(lactic-co-glycolic acid) particles for biomedical applications," *Acta Biomater.*, vol. 73, pp. 38–51, 2018.

[58] N. K. Varde, D. W. Pack, N. K. Varde, and D. W. Pack, "Microspheres for controlled release drug delivery Microspheres for controlled," vol. 2598, no. 2004, 2005.

[59] I. Ortega-oller, M. Padial-molina, P. Galindo-moreno, F. O. Valle, A. B. Jódar-reyes, and J. M. Peula-garcía, "Bone Regeneration from PLGA Micro-Nanoparticles," vol. 2015, no. 1, 2015.

[60] J. A. D. Sequeira, A. C. Santos, J. Serra, F. Veiga, and A. J. Ribeiro, "Poly(lactic-co-glycolic acid) (PLGA) matrix implants," *Nanostructures Eng. Cells, Tissues Organs From Des. to Appl.*, pp. 375–402, 2018.

[61] K. E. Uhrich, S. M. Cannizzaro, R. S. Langer, and K. M. Shakesheff, "Polymeric Systems for Controlled Drug Release," *Chem. Rev.*, vol. 99, no. 11, pp. 3181–3198, 1999.

[62] M. D. Blanco and M. J. Alonso, "Development and characterization of protein-loaded poly(lactide-co-glycolide) nanospheres," *European Journal of Pharmaceutics and Biopharmaceutics*, vol. 43, no. 3. pp. 287–294, 1997.

[63] P. W. Lee and J. K. Pokorski, "Poly(lactic-co-glycolic acid) devices: Production and applications for sustained protein delivery," *Wiley Interdiscip. Rev. Nanomedicine Nanobiotechnology*, vol. 10, no. 5, pp. 1–22, 2018.

[64] F. Ito, H. Fujimori, and K. Makino, "Factors affecting the loading efficiency of water-soluble drugs in PLGA microspheres," *Colloids Surfaces B Biointerfaces*, vol. 61, no. 1, pp. 25–29, 2008.

[65] L. Mu and S. S. Feng, "PLGA/TPGS Nanoparticles for Controlled Release of Paclitaxel: Effects of the Emulsifier and Drug Loading Ratio," *Pharm. Res.*, vol. 20, no. 11, pp. 1864–1872, 2003.

[66] T. Feczkó, J. Tóth, G. Dósa, and J. Gyenis, "Influence of process conditions on the mean size of PLGA nanoparticles," *Chem. Eng. Process. Process Intensif.*, vol. 50, no. 8, pp. 846–853, 2011.

[67] V. Filipe, A. Hawe, and W. Jiskoot, "Critical Evaluation of Nanoparticle Tracking Analysis (NTA) by NanoSight for the Measurement of Nanoparticles and Protein Aggregates," vol. 27, no. 5, pp.

796–810, 2010.

[68] J. 2006. T. Estey, J. Kang, S. P. Schwendeman, and J. F. Carpenter, “BSA degradation under acidic conditions: A model for protein instability during release from PLGA delivery systems,” Journal of Pharmaceutical Sciences, vol. 95, no. 7, pp. 1626–1639, “BSA degradation under acidic conditions: A model for protein instability during release from PLGA delivery systems,” *J. Pharm. Sci.*, vol. 101, no. 7, pp. 2271–2280, 2012.

[69] A. Lamprecht, N. Ubrich, M. Hombreiro Pérez, C. M. Lehr, M. Hoffman, and P. Maincent, “Influences of process parameters on nanoparticle preparation performed by a double emulsion pressure homogenization technique,” *Int. J. Pharm.*, vol. 196, no. 2, pp. 177–182, 2000.

CHAPTER 7: APPENDIX

The encapsulation efficacy of the Batch 4 PLGA nanoparticles was confirmed by HPLC. As the Batch 4 of the PLGA nanoparticles gave a 97.37% encapsulation efficacy with UV spectrophotometer, the drug content in the supernatant was determined by analyzing the sample in HPLC- Fluorescence as shown:

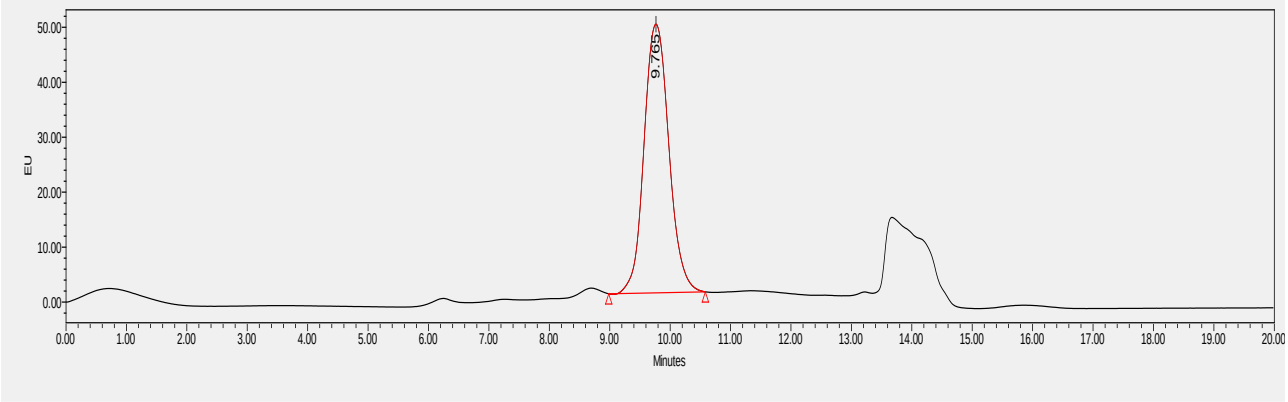

Figure 27: The drug content (BSA) in the supernatant after ultracentrifugation determined using HPLC-Fluorescence (RT – 9 to 10)

The retention time of the BSA is from 9 to 10 minutes. The sample concentration was assessed relative to a standard calibration curve of Bovine Serum Albumin (BSA) prepared in the mobile phase, and Absorbance = 13992785 was noted and concentration = 16.99639 µg/mL was determined using the calibration curve, and Encapsulation Efficiency was calculated to be 96.44%.

DRUG RELEASE – HPLC DATA

1. PLGA-BSA at 48 hours:

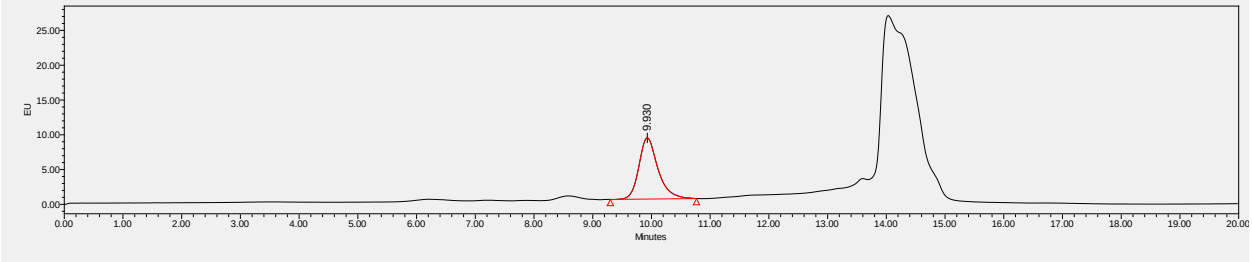

	Name	Retention Time	Area	% Area	Height	Int Type	Amount	Units
1		9.930	1988715	100.00	88080	bb		

2. PLGA-BSA-PNIPAAM at 48 hours:

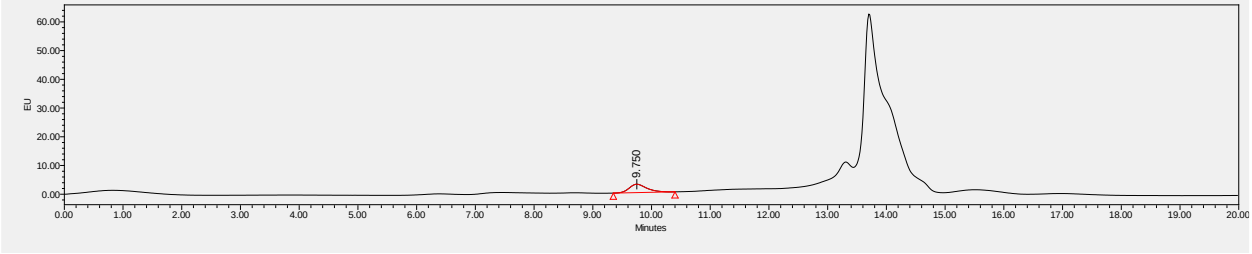

	Name	Retention Time	Area	% Area	Height	Int Type	Amount	Units
1		9.750	607772	100.00	29213	bb		